

Consensus over Clustered Networks Using Intermittent and Asynchronous Output Feedback

Federico M. Zegers and Sean Phillips

Abstract—In recent years, multi-agent teaming has garnered considerable interest since complex objectives, such as intelligence, surveillance, and reconnaissance, can be divided into multiple cluster-level sub-tasks and assigned to a cluster of agents with the appropriate functionality. Yet, coordination and information dissemination between clusters may be necessary to accomplish a desired objective. Distributed consensus protocols provide a mechanism for spreading information within clustered networks, allowing agents and clusters to make decisions without requiring direct access to the state of the ensemble. Hence, we propose a strategy for achieving system-wide consensus in the states of identical linear time-invariant systems coupled by an undirected graph whose directed sub-graphs are available only at sporadic times. Within this work, the agents of the network are organized into pairwise disjoint clusters, which induce sub-graphs of the undirected parent graph. Some cluster sub-graph pairs are linked by an inter-cluster sub-graph, where the union of all cluster and inter-cluster sub-graphs yields the undirected parent graph. Each agent utilizes a distributed consensus protocol with components that are updated intermittently and asynchronously with respect to other agents. The closed-loop ensemble dynamics is modeled as a hybrid system, and a Lyapunov-based stability analysis yields sufficient conditions for rendering the agreement subspace (consensus set) globally exponentially stable. Furthermore, an input-to-state stability argument demonstrates the consensus set is robust to a class of perturbations. A numerical simulation considering both nominal and perturbed scenarios is provided for validation purposes.

I. INTRODUCTION

A. Motivation

The Internet of Things (IoT) and advancements in data handling within network systems have created a paradigm shift in how the internet and distributed platforms are used today [1]. Consumer electronics and household devices such as cameras, watches, televisions, and refrigerators are now equipped with WiFi or LAN functionality granting the user access to nearly instantaneous data and wider control of their environment [2]. Connected devices, like those listed above, possess a natural graphical structure called a cluster-based network [3] or small-world network [4]–[6]. Although sophisticated, the technology enabling current small-world networks will need to evolve so that it can address imminent challenges. For instance, as more

devices gain internet connectivity and transmit more data due to improved capability, the resulting small-world networks will increase in complexity and require enhanced data handling and control protocols to meet demands. Bottlenecks introduced by finite network resources, e.g., bandwidth and throughput, and the need to perform control using limited information are ever-present constraints for multi-agent systems (MASs), especially those consisting of platforms with dynamics, such as vehicles.

Given their wide applicability and utility in coordination [7], we are interested in distributed consensus protocols for MASs. Specifically, we focus on consensus over clustered networks while utilizing intermittent and asynchronous output feedback. Data-handling protocols that embrace intermittency and asynchrony can better accommodate large-scale networks and data-dense exchanges than those using continuity and synchrony. Moreover, output feedback is an example of limited information. In practice, certain components of cyber-physical systems may operate at a constant rate, for example, electromechanical sensors and digital processors. Consequently, some information needed for control may be available periodically, motivating the development of controllers that leverage intermittent feedback to seamlessly integrate with such components. Moreover, intermittency can promote efficient resource utilization relative to legacy systems requiring continuous or periodic updates. The agents should also accommodate asynchronous information since delays in data propagation across networks and different operating tempos between agents occur naturally in distributed systems.

B. Background

The consensus problem for MASs, in both the continuous-time and discrete-time settings, has been well-studied in [8]. Furthermore, the survey papers in [9]–[11] provide additional information on MASs and consensus. Recently, however, there has been significant research on consensus where the communication between agents and control updates within agents are periodic, intermittent, and/or event-triggered [12]–[19]. These works were motivated by the efficient use of limited resources and the implementation challenges inherent to cyber-physical systems caused by, for example, sensor sampling rates, radio broadcast rates, and actuator constraints. Yet, there is a lack of research focusing on consensus over clustered networks, which is somewhat surprising since it is natural to solve complicated problems with cooperative teams of specialized agents. In fact, clustering in network systems is quite common in engineering applications [3], [20]–[24].

The results in [25]–[31] delve into the control of MASs over clustered networks. In [25], the authors develop a distributed

F. M. Zegers is with Johns Hopkins University Applied Physics Laboratory, Laurel, MD 20723, USA. E-mail: federico.zegers@jhuapl.edu.

S. Phillips is with the Air Force Research Laboratory, Space Vehicles Directorate, Kirtland AFB, NM 87117, USA. Approved for public release; distribution unlimited. Public Affairs approved AFRL-2024-3483.

This research is supported in part by the Office of Naval Research Grant N00014-21-1-2415; AFOSR award numbers FA9550-19-1-0169, FA9550-22-1-0429, and AFRL grant FA8651-21-F-1027. Any opinions, findings, conclusions, or recommendations expressed in this material are those of the author(s) and do not necessarily reflect the views of the sponsoring agencies.

controller enabling p -cluster consensus for a MAS of identical linear time-invariant (LTI) systems coordinating over a static or switching graph. Given a graph encoding a MAS whose vertex set is partitioned into p elements (i.e., clusters), p -cluster consensus is said to occur whenever the agents in each cluster achieve consensus, and the consensus value between clusters is distinct. Note that p -cluster consensus is accomplished using continuous state feedback. In [26], the authors investigate the formation control problem for clustered networks of identical LTI systems. The authors develop a distributed controller that enables M clusters to assemble distinct rigid formations using intermittent state feedback while compensating for communication delays.

The result in [27] presents a distributed consensus controller for a clustered network of identical LTI systems, where each agent leverages a mixture of continuous and intermittent output feedback. Each cluster is assigned a single leader, and, within each cluster, all agents may continuously communicate output information with their neighbors. However, only the leaders of each cluster may communicate intermittently with neighboring leaders, and this is the means by which information is spread across clusters. In addition, all leaders communicate with their neighboring leaders at the same isolated times. A Luenberger-like observer produces state estimates from output information, which are then used for control. Albeit not written, the analysis in [27] renders the agreement subspace for the entire ensemble globally exponentially stable. Leveraging analogous arguments and cluster structures found in [27], the result in [28] develops a distributed controller enabling a clustered network of identical LTI systems to assemble a single rigid formation using a mixture of continuous and intermittent state feedback. In [29], the authors build on the result of [25] and identify the general graph property that supports p -cluster consensus independent of coupling strength.

C. Comparison to Previous Work

In [30], we build on [27] and develop a distributed controller for a clustered network of identical LTI systems that enables consensus across the entire ensemble. Like [27], communication within clusters is continuous, and communication between clusters is intermittent. Nevertheless, unlike [27], there is no leader-follower structure in [30], and more general partitions of the communication graph are considered. As a result, more than one agent in a cluster can have a neighbor in a different cluster. Moreover, in [30], two pairs of distinct clusters may exchange information at different rates (i.e., asynchronously), unlike [27]. Still, it is important to observe that [27] considers output feedback while [30] only considers state feedback.

Our result in [31] is an extension of [30]. More precisely, [31] develops a distributed controller for a clustered network of identical LTI systems that enables ensemble-wide consensus using output feedback. Similar to the results in [27] and [30], communication in clusters is continuous, while communication between clusters is intermittent. Yet, rather than broadcast state information between neighbors as in [30], state estimates are broadcast instead, which are obtained using a Luenberger-like observer. This observer intermittently samples the output of an agent and leverages model knowledge and the control input to

compute a state estimate.

Unfortunately, the stability analysis in [31] suffers from an artificial defect. To demonstrate the desired set \mathcal{A} —which has the agreement subspace as a component—is globally exponentially stable, the stability analysis required all Luenberger-like observers to undergo synchronous jumps. The price to pay for this mathematical convenience is that all agents must synchronously sample their output, which is unreasonable for large-scale networks.

D. Contributions

Motivated by our previous work in [30], [31], we introduce a distributed consensus controller for a clustered network of identical LTI systems that uses intermittent and asynchronous output feedback. A connected, undirected, and static communication graph that is decomposed into connected, undirected, and static sub-graphs, with union returning the parent graph, defines the notion of clustered network within this work. These sub-graphs are separated into two groups, that is, clusters and inter-clusters, which are precisely defined in Section II. Each agent and inter-cluster is assigned a timer that dictates when measurement and control update events take place.

Within each cluster, each agent intermittently measures the outputs of their same-cluster neighbors and themselves when instructed by their timer mechanism. Similarly, within an inter-cluster, each agent intermittently measures the outputs of their same-inter-cluster neighbors and themselves when instructed by the inter-cluster timer mechanism. Such measurements may occur asynchronously between agents and inter-clusters. Thus, the measurement of output information is completely intermittent throughout the entire network, unlike [27], [30] and [31] which have components that use continuous communication to obtain output information.

The outputs are used to impulsively reset estimators, which evolve in an open-loop fashion during flows. The estimators replace the Luenberger-like observers from [31] and the need for explicit model knowledge in the controller. In addition, the controller utilizes the estimator outputs to facilitate consensus in the states of the LTI systems. To capture the continuous-time and discrete-time behaviors of the closed-loop ensemble system, we construct a hybrid model of the form in [32]. We also transform the consensus objective into a set stabilization problem for hybrid systems. A set \mathcal{A} , encoding the consensus subspace, is demonstrated to be globally exponentially stable using a Lyapunov-based stability analysis. The nominal well-posedness of the proposed hybrid system implies that the set \mathcal{A} is robust to vanishing perturbations. An input-to-state stability argument for hybrid systems is also provided to show that the set \mathcal{A} is robust to perturbations that are Lebesgue measurable and locally essentially bounded for the closed-loop hybrid system. Such an input-to-state stability argument cannot be found in [27], [30] and [31]. Lastly, we would like to stress that this work, as well as our previous works [30], [31], provide an alternative method of defining clustered networks and their associated sub-graphs when compared to the works in [25]–[29]. This particular construction is generic and facilitates the use of standard analysis techniques intended for traditional MASs. The theoretical development is validated in simulation,

where we provide an online path planner for a rendezvous application.

E. Organization

Section II provides information on notation, graphs, cluster and inter-cluster sub-graphs, and hybrid systems. Section III describes the specific problem we are aiming to solve. The proposed solution and closed-loop hybrid inclusion are presented in Section IV. In Section V, we provide the main results of the paper in the form of sufficient conditions for the nominal system and, in Section VI, we extend these results to consider the case of perturbations. Lastly, we illustrate the results through numerical simulations in Section VII.

II. PRELIMINARIES

A. Notation

Let \mathbb{R} and \mathbb{Z} denote the set of reals and integers, respectively. For a constant $a \in \mathbb{R}$, let $\mathbb{R}_{\geq a} \triangleq [a, \infty)$, $\mathbb{R}_{>a} \triangleq (a, \infty)$, $\mathbb{Z}_{\geq a} \triangleq \mathbb{R}_{\geq a} \cap \mathbb{Z}$, and $\mathbb{Z}_{>a} \triangleq \mathbb{R}_{>a} \cap \mathbb{Z}$. For $p, q \in \mathbb{Z}_{>0}$, the $p \times q$ zero matrix and the $p \times 1$ zero column vector are respectively denoted by $0_{p \times q}$ and 0_p . The $p \times p$ identity matrix and the $p \times 1$ column vector with all entries being one are denoted by I_p and 1_p , respectively. The Euclidean norm of $r \in \mathbb{R}^p$ is denoted by $\|r\| \triangleq \sqrt{r^\top r}$. For $x, y \in \mathbb{R}^p$, the inner product between x and y is denoted by $\langle x, y \rangle \triangleq x^\top y$. For $M \in \mathbb{Z}_{\geq 2}$, let $[M] \triangleq \{1, 2, \dots, M\}$. The Kronecker product between $A \in \mathbb{R}^{p \times q}$ and $B \in \mathbb{R}^{u \times v}$, where $u, v \in \mathbb{Z}_{>0}$, is denoted by $A \otimes B \in \mathbb{R}^{pu \times qv}$. The maximum and minimum eigenvalues of a real symmetric matrix $A \in \mathbb{R}^{n \times n}$ are denoted by $\lambda_{\max}(A)$ and $\lambda_{\min}(A)$, respectively. The block diagonal matrix with general blocks G_1, G_2, \dots, G_p is denoted by $\text{diag}(G_1, G_2, \dots, G_p)$. The distance of a point $r \in \mathbb{R}^p$ to the set $S \subset \mathbb{R}^p$ is given by $|r|_S \triangleq \inf\{\|r - s\| : s \in S\} \in \mathbb{R}_{\geq 0}$; furthermore, define the set addition property as $r + S \triangleq \{r + s \in \mathbb{R}^p : s \in S\}$. For a collection of vectors $\{z_1, z_2, \dots, z_p\} \subset \mathbb{R}^q$, let $(z_k)_{k \in [p]} \triangleq [z_1^\top, z_2^\top, \dots, z_p^\top]^\top \in \mathbb{R}^{pq}$. Similarly, for $x \in \mathbb{R}^p$ and $y \in \mathbb{R}^q$, let $(x, y) \triangleq [x^\top, y^\top]^\top \in \mathbb{R}^{p+q}$. For any sets A and B , a function f of A with values in B is denoted by $f: A \rightarrow B$, whereas $f: A \rightrightarrows B$ refers to a set-valued function $f: A \rightarrow 2^B$. The k^{th} standard basis vector of \mathbb{R}^N , for $N \in \mathbb{Z}_{>0}$, is denoted by e_k . Similarly, let \tilde{e}_k denote the k^{th} standard basis vector of \mathbb{R}^{N-1} . The range (i.e., image) of a matrix $A \in \mathbb{R}^{N \times N}$ is denoted by $\text{Range}(A) \triangleq \{y \in \mathbb{R}^N : y = Ax \text{ for some } x \in \mathbb{R}^N\}$. For any $x \in \mathbb{R}$, let $\lfloor x \rfloor \triangleq \sup\{c \in \mathbb{Z} : c \leq x\}$.

B. Graphs

Let $\mathcal{G} \triangleq (\mathcal{V}, \mathcal{E})$ be a graph on $N \in \mathbb{Z}_{\geq 2}$ nodes, where $\mathcal{V} \triangleq [N]$ denotes the node set and $\mathcal{E} \subseteq \mathcal{V} \times \mathcal{V}$ denotes the edge set. If $(p, q) \in \mathcal{E}$ implies $(q, p) \in \mathcal{E}$ for all distinct nodes $p, q \in \mathcal{V}$, then the graph \mathcal{G} is said to be undirected. A path exists between nodes $p, q \in \mathcal{V}$ if there is a sequence of distinct nodes such that $(v_0 = p, \dots, v_k = q)$ for $k \in \mathbb{Z}_{\geq 0}$, $(v_{s-1}, v_s) \in \mathcal{E}$, and $s \in [k]$. The graph \mathcal{G} is said to be connected if there is a path joining any two distinct nodes in \mathcal{V} . The neighbor set of node p is denoted by $\mathcal{N}_p \triangleq \{q \in \mathcal{V} \setminus \{p\} : (p, q) \in \mathcal{E}\}$. The adjacency matrix of \mathcal{G} is denoted by $A \triangleq [a_{pq}] \in \mathbb{R}^{N \times N}$, where $a_{pq} = 1$ if and only if $(p, q) \in \mathcal{E}$, and $a_{pq} = 0$ otherwise. Self-edges are

not employed in this work, that is, $a_{pp} \triangleq 0$ for all $p \in \mathcal{V}$. The degree matrix of \mathcal{G} is denoted by $\Delta \triangleq \text{diag}(A \cdot 1_N) \in \mathbb{R}^{N \times N}$. The Laplacian matrix of \mathcal{G} is denoted by $L \triangleq \Delta - A \in \mathbb{R}^{N \times N}$. The following result enables the stability analysis provided in Section V.

Lemma 1. If \mathcal{G} is static, undirected, and connected, then there exists an orthonormal basis $\beta \triangleq \{v_1, v_2, \dots, v_N\} \subset \mathbb{R}^N$ for $\text{Range}(L)$ such that $v_1 = (\sqrt{N}/N)1_N$. Consider the matrix $V \triangleq [v_2, v_3, \dots, v_N] \in \mathbb{R}^{N \times N-1}$ and projection $S \triangleq I_N - 1_N 1_N^\top / N \in \mathbb{R}^{N \times N}$. Then,

$$L = VDV^\top, \quad V^\top V = I_{N-1}, \quad \text{and} \quad (1)$$

$$S = VV^\top \quad (2)$$

for some diagonal, positive definite $D \in \mathbb{R}^{N-1 \times N-1}$. \triangle

The matrix S is a projection whose image is the orthogonal complement of the agreement subspace $\text{Span}(1_N)$. That is, for any vector $z \in \mathbb{R}^N$, z may be decomposed into the sum of two orthogonal vectors, i.e., $z = z^\parallel + z^\perp$, where $z^\parallel \triangleq (1_N 1_N^\top / N)z$ and $z^\perp \triangleq Sz$. In addition, for any symmetric Laplacian matrix \mathcal{L} , one can show by direct computation that $S\mathcal{L} = \mathcal{L} = \mathcal{L}S$.

Proof of Lemma 1. See Appendix A. \blacksquare

C. Cluster and Inter-Cluster Sub-Graphs

Let $\mathcal{G} = (\mathcal{V}, \mathcal{E})$ be a static, undirected, and connected graph. Let $\mathcal{C}(\mathcal{V}) \triangleq \{\mathcal{V}_1, \mathcal{V}_2, \dots, \mathcal{V}_M\}$ be a fixed partition of the set \mathcal{V} , where $M \in [N]$ is some constant. Consequently, $\mathcal{V}_p \subseteq \mathcal{V}$ for each $p \in [M]$, $\mathcal{V}_p \cap \mathcal{V}_q = \emptyset$ for each distinct pair $p, q \in [M]$, and $\cup_{p \in [M]} \mathcal{V}_p = \mathcal{V}$. The sets $\mathcal{C}(\mathcal{V})$ and \mathcal{V}_q , for any $q \in \mathcal{V}$, are referred to as the *cluster set of \mathcal{G}* and *cluster q* , respectively. Since $\mathcal{C}(\mathcal{V})$ is an arbitrary partition of \mathcal{V} , for every $p \in [M]$, cluster p contains at least one node, i.e., $|\mathcal{V}_p| \geq 1$. Each cluster induces a sub-graph of \mathcal{G} , i.e., for each $p \in [M]$, the induced sub-graph of cluster p is given by $\mathcal{G}[\mathcal{V}_p] \triangleq (\mathcal{V}_p, \mathcal{E}[\mathcal{V}_p])$, such that $\mathcal{E}[\mathcal{V}_p] \triangleq \{(r, s) \in \mathcal{E} : r, s \in \mathcal{V}_p\}$. Since \mathcal{G} is undirected, $\mathcal{G}[\mathcal{V}_p]$ is undirected. In this work, we only consider cluster sets $\mathcal{C}(\mathcal{V})$ where, for each $p \in [M]$, $\mathcal{G}[\mathcal{V}_p]$ is connected. Moreover, since $\mathcal{C}(\mathcal{V})$ is a fixed partition of \mathcal{V} , for each $p \in \mathcal{V}$, node p is assigned to one cluster for all time. In particular, for each $p \in \mathcal{V}$, let \mathcal{C}_p denote the cluster to which node p belongs, i.e., $p \in \mathcal{C}_p$ and $\mathcal{C}_p = \mathcal{V}_q$ for some $\mathcal{V}_q \in \mathcal{C}(\mathcal{V})$. The set of neighbors of node p within \mathcal{C}_p is, therefore, given by $\mathcal{N}_p \cap \mathcal{C}_p$.

For any distinct pair $p, q \in [M]$, let $\mathcal{V}_{pq} \triangleq \mathcal{V}(p, q) \cup \mathcal{V}(q, p)$, such that $\mathcal{V}(p, q) \triangleq \{r \in \mathcal{V}_p : \exists s \in \mathcal{V}_q (r, s) \in \mathcal{E}\}$. If $\mathcal{V}_{pq} \neq \emptyset$, then the set \mathcal{V}_{pq} is referred to as *inter-cluster pq* . To simplify the development, we only consider the case where there is at most one inter-cluster between each pair of distinct clusters. The *inter-cluster set of \mathcal{G}* , as determined by $\mathcal{C}(\mathcal{V})$, is denoted by $\mathcal{I}(\mathcal{V}) \triangleq \{\mathcal{V}_{pq} \subset \mathcal{V} : \forall p \neq q \in \mathcal{V} \mathcal{V}_{pq} \neq \emptyset\}$. Since $|\mathcal{C}(\mathcal{V})| = M$ and there can be at most one inter-cluster between each distinct pair of clusters, $|\mathcal{I}(\mathcal{V})| = M^* \in \{0, 1, \dots, M(M-1)/2\}$. For each distinct pair of $p, q \in [M]$, the sub-graph of \mathcal{G} induced by inter-cluster pq is denoted by $\mathcal{G}[\mathcal{V}_{pq}] \triangleq (\mathcal{V}_{pq}, \mathcal{E}_{pq})$, where $\mathcal{E}_{pq} \triangleq \mathcal{E}[\mathcal{V}_{pq}] \setminus (\mathcal{E}[\mathcal{V}_p] \cup \mathcal{E}[\mathcal{V}_q])$. Further, $\mathcal{G}[\mathcal{V}_{pq}]$ is undirected by construction. Figure 1 illustrates an example of a graph \mathcal{G} that is divided into cluster and inter-cluster sub-graphs. Since $\mathcal{C}(\mathcal{V})$ and \mathcal{G} are fixed, one has that $\mathcal{I}(\mathcal{V})$ is fixed as well. Thus,

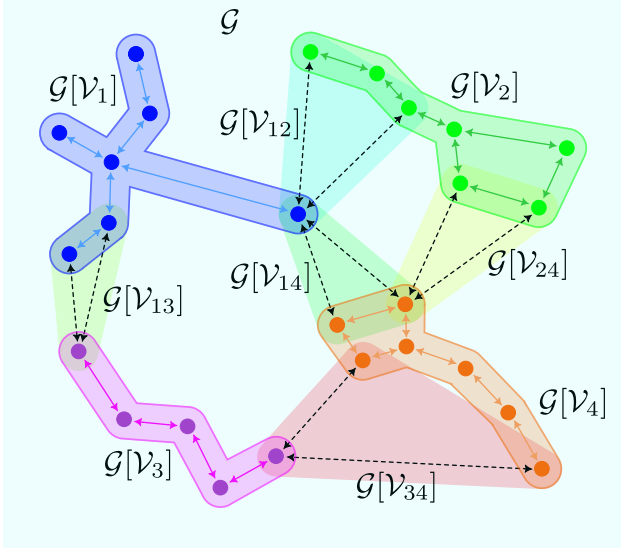


Figure 1: Within the undirected graph \mathcal{G} , as denoted by the disks and double-headed arrows, there are four sub-graphs induced by clusters and five sub-graphs induced by inter-cluster. Note that solid arrows represent edges within clusters, while dashed arrows represent edges between clusters, i.e., within inter-clusters. The cluster sub-graphs of \mathcal{G} are $\mathcal{G}[\mathcal{V}_1]$, $\mathcal{G}[\mathcal{V}_2]$, $\mathcal{G}[\mathcal{V}_3]$, and $\mathcal{G}[\mathcal{V}_4]$. The inter-cluster sub-graphs of \mathcal{G} are $\mathcal{G}[\mathcal{V}_{12}]$, $\mathcal{G}[\mathcal{V}_{13}]$, $\mathcal{G}[\mathcal{V}_{14}]$, $\mathcal{G}[\mathcal{V}_{24}]$, and $\mathcal{G}[\mathcal{V}_{34}]$. By construction, the union of all sub-graphs returns the original graph \mathcal{G} .

if node $p \in \mathcal{V}$ belongs to an inter-cluster, then it does so for all time. Moreover, it is possible for a node to belong to multiple inter-clusters simultaneously. The set of neighbors of node p in inter-cluster rs is, therefore, given by $\mathcal{N}_p \cap \mathcal{V}_{rs}$.

To facilitate the analysis, $N \times N$ augmented adjacency and Laplacian matrices for a general sub-graph of \mathcal{G} are introduced next. For any non-empty set $S \subseteq \mathcal{V}$, let $A[S] \triangleq [a_{pq}] \in \mathbb{R}^{N \times N}$ with

$$a_{pq} \triangleq \begin{cases} 1, & (p, q) \in \mathcal{E}[S] \\ 0, & \text{otherwise} \end{cases}$$

denote the augmented adjacency matrix of $\mathcal{G}[S]$. Therefore, the augmented adjacency matrix of cluster p and inter-cluster pq are $A[\mathcal{V}_p]$ and $A[\mathcal{V}_{pq}]$, respectively. Each augmented adjacency matrix has a corresponding augmented Laplacian matrix. The augmented Laplacian matrix of $S \subseteq \mathcal{V}$ is $L[S] \triangleq \text{diag}(A[S] \cdot \mathbf{1}_N) - A[S] \in \mathbb{R}^{N \times N}$. Consequently, the augmented Laplacian matrix of cluster p and inter-cluster pq are $L[\mathcal{V}_p]$ and $L[\mathcal{V}_{pq}]$, respectively.

For convenience, we introduce and henceforth use an alternative labeling scheme for the inter-clusters of \mathcal{G} as determined by a cluster set $\mathcal{C}(\mathcal{V})$. Let $\mathfrak{b}: [M] \times [M] \rightarrow [M^*]$ be a bijection. Given a cluster set $\mathcal{C}(\mathcal{V})$ with cardinality M , there are exactly M^* pairs of distinct clusters with an inter-cluster. Hence, for some $p, q \in [M]$ with $p \neq q$, there exists a unique $r \in [M^*]$ such that $\mathfrak{b}(p, q) = r$. By inductively using the bijection \mathfrak{b} , let $\mathcal{V}^r \triangleq \mathcal{V}_{pq}$ for all $p, q \in [M]$ with $p \neq q$ such that $\mathfrak{b}(p, q) = r$. Thus, the sub-graph and augmented Laplacian matrix of inter-cluster pq , for example, can also be written as $\mathcal{G}[\mathcal{V}^r]$ and $L[\mathcal{V}^r]$, respectively. A static, undirected, and connected graph \mathcal{G} with

cluster and inter-cluster sub-graphs determined by cluster set $\mathcal{C}(\mathcal{V})$ and inter-cluster set $\mathcal{I}(\mathcal{V})$, respectively, is henceforth referred to as *clustered network*.

For each $p \in \mathcal{V}$, the neighbor set of agent p , that is, \mathcal{N}_p , can be partitioned using the cluster set $\mathcal{C}(\mathcal{V})$ and inter-cluster set $\mathcal{I}(\mathcal{V})$. The partition of \mathcal{N}_p is given by $\mathcal{N}_p \triangleq \{\mathcal{N}_p \cap \mathcal{C}_p, \mathcal{N}_p \cap \mathcal{V}^1, \mathcal{N}_p \cap \mathcal{V}^2, \dots, \mathcal{N}_p \cap \mathcal{V}^{M^*}\}$, where $S_1 \cap S_2 = \emptyset$ for any distinct $S_1, S_2 \in \mathcal{N}_p$ and

$$\mathcal{N}_p = (\mathcal{N}_p \cap \mathcal{C}_p) \cup \left(\bigcup_{r \in [M^*]} (\mathcal{N}_p \cap \mathcal{V}^r) \right). \quad (3)$$

Note, for any connected graph \mathcal{G} , it may be possible for $\mathcal{N}_p \cap \mathcal{C}_p = \emptyset$ for some agent $p \in \mathcal{V}$ and/or $\mathcal{N}_p \cap \mathcal{V}^r = \emptyset$ for some inter-cluster $r \in [M^*]$.

D. Hybrid Systems

A hybrid system \mathcal{H} with data (C, f, D, G) is defined as

$$\mathcal{H}: \begin{cases} \dot{\xi} = f(\xi), & \xi \in C \\ \xi^+ \in G(\xi), & \xi \in D, \end{cases}$$

where $f: \mathbb{R}^n \rightarrow \mathbb{R}^n$ denotes the flow map, $C \subset \mathbb{R}^n$ denotes the flow set, $G: \mathbb{R}^n \rightrightarrows \mathbb{R}^n$ denotes the jump map, and $D \subset \mathbb{R}^n$ denotes the jump set. A set $\Omega \subset \mathbb{R}_{\geq 0} \times \mathbb{Z}_{\geq 0}$ is a hybrid time domain, if there is a non-decreasing sequence of non-negative reals $(t_j)_{j=0}^m$ with $m \in \mathbb{Z}_{\geq 0} \cup \{\infty\}$, $t_0 = 0$, and $t_m \in \mathbb{R}_{\geq 0} \cup \{\infty\}$, such that $\Omega = \bigcup_{j=1}^m (I_j \times \{j-1\})$, where all the intervals I_j , for $j < m$, are of the form $[t_{j-1}, t_j]$, and I_m is of the form $[t_{m-1}, t_m]$ or $[t_{m-1}, t_m)$ when $m < \infty$. Note that $t_m = \infty$ is allowed when $m < \infty$; for $m = \infty$ there is no t_m . The time t_j indicates the j^{th} instant the state ξ jumps, where the value of ξ after a jump is denoted by ξ^+ . A hybrid arc ϕ is a function $\phi: \text{dom } \phi \rightarrow \mathbb{R}^n$, such that $\text{dom } \phi \subset \mathbb{R}_{\geq 0} \times \mathbb{Z}_{\geq 0}$ is a hybrid time domain with jump sequence $(t_j)_{j=0}^m$, and ϕ is a locally absolutely continuous function on I_j , for every j . A solution of \mathcal{H} is a hybrid arc ϕ such that, for all $j > 0$, $\phi(t, j-1) \in C$ and $\dot{\phi}(t, j-1) = f(\phi(t, j-1))$ for almost all $t \in I_j$; and $\phi(t_{j-1}, j-1) \in D$ and $\phi(t_{j-1}, j) \in G(\phi(t_{j-1}, j-1))$. A solution ϕ to \mathcal{H} is called maximal if ϕ cannot be extended, i.e., there does not exist a distinct solution ψ to \mathcal{H} such that $\text{dom } \phi \subseteq \text{dom } \psi$ and $\phi(t, j) = \psi(t, j)$ for all $(t, j) \in \text{dom } \phi$. A solution ϕ is called complete if $\text{dom } \phi$ is unbounded. A hybrid system \mathcal{H} with data (C, f, D, G) is said to satisfy the hybrid basic conditions if it satisfies [32, Assumption 6.5]. The following definition originates from [33, Section II].

Definition 1. Let \mathcal{H} be a hybrid system on $\mathcal{X} \subset \mathbb{R}^n$ with data (C, f, D, G) . A closed set $\mathcal{A} \subset \mathcal{X}$ is said to be *globally exponentially stable* (GES) for the hybrid system \mathcal{H} if there exist constants $\kappa, \alpha \in \mathbb{R}_{>0}$ such that every maximal solution ϕ of \mathcal{H} is complete and satisfies

$$|\phi(t, j)|_{\mathcal{A}} \leq \kappa \exp(-\alpha(t+j)) |\phi(0, 0)|_{\mathcal{A}}$$

for all $(t, j) \in \text{dom } \phi$. \triangle

When considering perturbations on \mathcal{H} , input-to-state stability (ISS) is a useful analysis tool. The following definition comes from [34, Definition 2.2].

Definition 2. The hybrid system with state z and input u given by

$$\begin{aligned} \dot{z} &= f(z, u), & (z, u) &\in C \\ z^+ &\in G(z, u), & (z, u) &\in D \end{aligned} \quad (4)$$

is said to be ISS with respect to a compact set \mathcal{A} if there exist $\beta \in \mathcal{KL}^1$ and $\gamma \in \mathcal{K}^2$ such that, for each $\phi(0, 0) \in \mathbb{R}^n$, every solution pair (ϕ, u) satisfies

$$|\phi(t, j)|_{\mathcal{A}} \leq \max\{\beta(|\phi(0, 0)|_{\mathcal{A}}, t + j), \gamma(|u|_{\infty})\}$$

for all $(t, j) \in \text{dom } \phi$. \triangle

Observe (ϕ, u) is a solution pair of (4) if, for each $j \in \mathbb{Z}_{\geq 0}$, the map $t \mapsto \phi(t, j)$ is locally absolutely continuous, $t \mapsto u(t, j)$ is Lebesgue measurable and locally essentially bounded over $\{t: (t, j) \in \text{dom}(\phi, u)\}$, $\text{dom } \phi = \text{dom } u$ where $\text{dom}(\phi, u) \triangleq \text{dom } \phi$ represents the hybrid time domain of (ϕ, u) , $(\phi(t, j-1), u(t, j-1)) \in C$ and $\dot{\phi}(t, j-1) = f(\phi(t, j-1), u(t, j-1))$ for almost all $t \in I_j$, and $(\phi(t_{j-1}, j-1), u(t_{j-1}, j-1)) \in D$ and $\phi(t_{j-1}, j) \in G(\phi(t_{j-1}, j-1), u(t_{j-1}, j-1))$. Note that the \mathcal{L}_{∞} norm, i.e., $|\cdot|_{\infty}$, is defined in [35, Section II].

III. PROBLEM FORMULATION

Consider a MAS of $N \in \mathbb{Z}_{\geq 2}$ agents, which are enumerated by the elements of \mathcal{V} . The motion model of agent $p \in \mathcal{V}$ is

$$\dot{x}_p = Ax_p + Bu_p, \quad y_p = Hx_p, \quad (5)$$

where $x_p \in \mathbb{R}^n$, $u_p \in \mathbb{R}^d$, and $y_p \in \mathbb{R}^m$ are the state variable, control input, and output of the agent, respectively. In addition, $A \in \mathbb{R}^{n \times n}$, $B \in \mathbb{R}^{n \times d}$, and $H \in \mathbb{R}^{m \times n}$ represent the known state, control effectiveness, and output matrices, respectively. To facilitate cooperation, the agents may exchange information via an intermittently available communication network, which is modeled by a static, undirected, and connected graph $\mathcal{G} = (\mathcal{V}, \mathcal{E})$ with cluster set $\mathcal{C}(\mathcal{V})$ and inter-cluster set $\mathcal{I}(\mathcal{V})$. Thus, \mathcal{G} possesses M cluster sub-graphs, i.e., $\{\mathcal{G}[\mathcal{V}_p]\}_{p \in [M]}$, and M^* inter-cluster sub-graphs, i.e., $\{\mathcal{G}[\mathcal{V}^r]\}_{r \in [M^*]}$. Further, for each $p \in \mathcal{V}$, agent p can measure the outputs of its neighbors and itself, that is, agent p can measure $\{y_q\}_{q \in \mathcal{N}_p \cup \{p\}}$.

The objective of this work is to develop a distributed controller for each agent $p \in \mathcal{V}$ that yields consensus in the agents' states, that is, $x_p = x_q$ for all distinct $p, q \in \mathcal{V}$. In addition, for each $p \in \mathcal{V}$, the controller of agent p should only utilize intermittent measurements of the outputs in $\{y_q\}_{q \in \mathcal{N}_p \cup \{p\}}$, which may be obtained asynchronously. To be more precise, the measurements of outputs belonging to agents in $\mathcal{N}_p \cap \mathcal{C}_p$, $\mathcal{N}_p \cap \mathcal{V}^r$, and $\mathcal{N}_p \cap \mathcal{V}^s$, for $r \neq s \in [M^*]$ with $\mathcal{N}_p \cap \mathcal{V}^r \neq \emptyset$ and $\mathcal{N}_p \cap \mathcal{V}^s \neq \emptyset$, may occur at different moments in time and at different rates. Such a control strategy better leverages limited resources relative to continuous communication and/or sensing alternatives, readily integrates in digital hardware, and accommodates the natural asynchronous flow of information within MASs.

¹A continuous function $\beta: \mathbb{R}_{\geq 0} \times \mathbb{R}_{\geq 0} \rightarrow \mathbb{R}_{\geq 0}$ belongs to class \mathcal{KL} if 1) $\beta(r, s)$ is non-decreasing in r , 2) $\lim_{r \rightarrow 0^+} \beta(r, s) = 0$ for each fixed $s \in \mathbb{R}_{\geq 0}$, 3) $\beta(r, s)$ is non-increasing in s , and 4) $\lim_{s \rightarrow \infty} \beta(r, s) = 0$ for each fixed $r \in \mathbb{R}_{\geq 0}$.

²A continuous function $\gamma: [0, a] \rightarrow \mathbb{R}_{\geq 0}$ with $a > 0$ belongs to class \mathcal{K} if 1) γ is strictly increasing and 2) $\gamma(0) = 0$.

IV. HYBRID SYSTEM DEVELOPMENT

For each $p \in \mathcal{V}$, let $0 < T_1^p \leq T_2^p$ be user-defined constants. Furthermore, let $\tau_p \in [0, T_2^p]$ be a timer for agent p that evolves according to the hybrid system

$$\begin{aligned} \dot{\tau}_p &= -1, & \tau_p &\in [0, T_2^p] \\ \tau_p^+ &\in [T_1^p, T_2^p], & \tau_p &= 0 \end{aligned} \quad (6)$$

with initial condition $\tau_p(0, 0) \in [0, T_2^p]$.³ The hybrid dynamics in (6) enables the construction of increasing sequences of time, e.g., $\{t_k^p\}_{k=0}^{\infty}$, given a complete solution ϕ_{τ_p} ,⁴ where the event time t_k^p represents the k^{th} instant $\tau_p = 0$. Moreover, the event times satisfy the following inequalities: for all $k \in \mathbb{Z}_{\geq 1}$,

$$T_1^p \leq t_{k+1}^p - t_k^p \leq T_2^p.$$

Likewise, for every inter-cluster $r \in [M^*]$, let $0 < T_3^r \leq T_4^r$ be user-defined constants, and let $\rho_r \in [0, T_4^r]$ be a timer for \mathcal{V}^r that evolves according to the hybrid system

$$\begin{aligned} \dot{\rho}_r &= -1, & \rho_r &\in [0, T_4^r] \\ \rho_r^+ &\in [T_3^r, T_4^r], & \rho_r &= 0 \end{aligned} \quad (7)$$

with initial condition $\rho_r(0, 0) \in [0, T_4^r]$. The hybrid dynamics in (7) enables the construction of increasing sequences of time, e.g., $\{t_k^r\}_{k=0}^{\infty}$, given a complete solution ϕ_{ρ_r} , where the event time t_k^r represents the k^{th} instant $\rho_r = 0$. Moreover, the event times satisfy the following inequalities: for all $k \in \mathbb{Z}_{\geq 1}$,

$$T_3^r \leq t_{k+1}^r - t_k^r \leq T_4^r.$$

These timers can be treated as independent autonomous systems that trigger certain actions. In particular, τ_p will be used to dictate when agent p obtains output information from same-cluster neighbors, and ρ_r will be used to determine when the agents in inter-cluster r obtain output information from same-inter-cluster neighbors.

For every agent $p \in \mathcal{V}$ and inter-cluster $r \in [M^*]$, let $\eta_p \in \mathbb{R}^m$ and $\zeta_{pr} \in \mathbb{R}^m$ be auxiliary variables that evolve according to

$$\begin{aligned} \dot{\eta}_p &= K_{\eta, p} \eta_p, & \tau_p &\in [0, T_2^p] \\ \eta_p^+ &= \sum_{q \in \mathcal{N}_p \cap \mathcal{C}_p} (y_q - y_p), & \tau_p &= 0 \end{aligned} \quad (8)$$

and

$$\begin{aligned} \dot{\zeta}_{pr} &= K_{\zeta, pr} \zeta_{pr}, & \rho_r &\in [0, T_4^r] \\ \zeta_{pr}^+ &= \sum_{q \in \mathcal{N}_p \cap \mathcal{V}^r} (y_q - y_p), & \rho_r &= 0, \end{aligned} \quad (9)$$

respectively, where $K_{\eta, p}, K_{\zeta, pr} \in \mathbb{R}^{m \times m}$ are user-defined matrices. Loosely speaking, a solution to (6) and (8) would yield an approximation of the consensus-like term $\sum_{q \in \mathcal{N}_p \cap \mathcal{C}_p} (y_q - y_p)$ given continuous-time trajectories for $\{y_q\}_{q \in \mathcal{N}_p \cap \mathcal{C}_p}$. The approximation is intermittently reset to the corresponding value of $\sum_{q \in \mathcal{N}_p \cap \mathcal{C}_p} (y_q - y_p)$ and allowed to flow in an open-loop fashion according to the flow equation in (8). Note that if $0 < T_1^p < T_2^p$, then the times when $\sum_{q \in \mathcal{N}_p \cap \mathcal{C}_p} (y_q - y_p)$ is sampled are intermittent since the timer may be reset to

³Examples that leverage the timer mechanism in (6) can be found in [17], [32], and [36].

⁴Note, ϕ_{τ_p} represents the value of τ_p along a solution ϕ of (6).

any number in the interval $[T_1^p, T_2^p]$. Periodic sampling can be created by selecting $0 < T_1^p = T_2^p$. An analogous comment follows for (7) and (9).

Given a user-defined matrix $K_u \in \mathbb{R}^{d \times m}$, the controller of agent p is

$$u_p \triangleq K_u \left(\eta_p + \sum_{r \in [M^*]} \zeta_{pr} \right) \in \mathbb{R}^d. \quad (10)$$

By construction, the controller in (10) is distributed as it only requires output information from neighboring agents and the implementing agent itself. Also, the output measurements are obtained intermittently, provided $T_1^p < T_2^p$ and $T_3^r < T_4^r$ for all $r \in [M^*]$, and the output measurements belonging to agents in $\mathcal{N}_p \cap \mathcal{C}_p$, $\mathcal{N}_p \cap \mathcal{V}^r$, and $\mathcal{N}_p \cap \mathcal{V}^s$, for $r \neq s \in [M^*]$, may be obtained asynchronously. Note the timer τ_p determines when agent p samples the data in $\{y_q - y_p\}_{q \in \mathcal{N}_p \cap \mathcal{C}_p}$ and updates the η_p component of its controller given (8). Likewise, the timer ρ_r determines when agent p samples the data in $\{y_q - y_p\}_{q \in \mathcal{N}_p \cap \mathcal{V}^r}$ and updates the ζ_{pr} component of its controller given (9). If agent p is not a member of inter-cluster r (i.e., $p \notin \mathcal{V}^r$), $\zeta_{pr} \equiv 0_m$. To facilitate the derivation of the closed-loop ensemble hybrid system, let

$$\tilde{\eta}_p \triangleq \eta_p - \sum_{q \in \mathcal{N}_p \cap \mathcal{C}_p} (y_q - y_p) \in \mathbb{R}^m, \quad (11)$$

$$\tilde{\zeta}_{pr} \triangleq \zeta_{pr} - \sum_{q \in \mathcal{N}_p \cap \mathcal{V}^r} (y_q - y_p) \in \mathbb{R}^m. \quad (12)$$

We provide the following notation to aid the writing of concise expressions. Let

$$\begin{aligned} x &\triangleq (x_p)_{p \in \mathcal{V}} \in \mathbb{R}^{nN}, & \eta &\triangleq (\eta_p)_{p \in \mathcal{V}} \in \mathbb{R}^{mN}, \\ \zeta_r &\triangleq (\zeta_{pr})_{p \in \mathcal{V}} \in \mathbb{R}^{mN}, & \zeta &\triangleq (\zeta_r)_{r \in [M^*]} \in \mathbb{R}^{mNM^*}, \\ \tilde{\eta} &\triangleq (\tilde{\eta}_p)_{p \in \mathcal{V}} \in \mathbb{R}^{mN}, & \tilde{\zeta}_r &\triangleq (\tilde{\zeta}_{pr})_{p \in \mathcal{V}} \in \mathbb{R}^{mN}, \\ \tilde{\zeta} &\triangleq (\tilde{\zeta}_r)_{r \in [M^*]} \in \mathbb{R}^{mNM^*}, & \tau &\triangleq (\tau_p)_{p \in \mathcal{V}} \in \mathbb{R}^N, \\ \rho &\triangleq (\rho_r)_{r \in [M^*]} \in \mathbb{R}^{M^*}. \end{aligned}$$

The substitution of the output equation in (5) and (10)–(12) into the differential equation in (5) yields

$$\begin{aligned} \dot{x}_p &= Ax_p + BK_u H \sum_{q \in \mathcal{N}_p} (x_q - x_p) + BK_u \sum_{r \in [M^*]} \tilde{\zeta}_{pr} \\ &\quad + BK_u \tilde{\eta}_p, \end{aligned} \quad (13)$$

where the summation term over the neighbor set of agent p is due to (3). Substituting (13) into the time derivative of x for each $p \in \mathcal{V}$ yields

$$\begin{aligned} \dot{x} &= ((I_N \otimes A) - (L \otimes BK_u H))x + (I_N \otimes BK_u) \tilde{\eta} \\ &\quad + (I_N \otimes BK_u)(1_{M^*}^\top \otimes I_{mN}) \tilde{\zeta}. \end{aligned} \quad (14)$$

Recall the objective, that is, drive x from any initial condition to a configuration where $x_p = x_q$ for all distinct $p, q \in \mathcal{V}$. Since any configuration x can be decomposed into orthogonal components, where $x = x^\parallel + x^\perp$, $x^\parallel \triangleq ((1_N 1_N^\top)/N \otimes I_n)x$ is the part of x in consensus, and $x^\perp \triangleq (S \otimes I_n)x$ is the part of x in dissensus, one can achieve the objective by driving $\|x^\perp\|$ to 0. Naturally, we attempted to produce a GES result using the dynamics of x^\perp . However, in this particular setting, such an

exercise was unfruitful because of the interaction between the non-trivial kernel of L and the linear time-invariant dynamics in (5).

The use of $SL = LS$ and the substitution of (14) into the time derivative of x^\perp yields a linear ordinary differential equation (ODE) that depends on the variable $(x^\perp, \tilde{\eta}, \tilde{\zeta})$. The matrix that pre-multiplies x^\perp cannot, in general, be made into a stability matrix through the selection of K_u , unless A itself is a stability matrix. Fortunately, Lemma 1 enables the succeeding result, which motivates the analysis of an alternative ODE.

Lemma 2. For any $z \in \mathbb{R}^{nN}$, $\|z^\perp\| = \|(V^\top \otimes I_n)z\|$. \triangle

Proof. By Lemma 1, $S = VV^\top$. Moreover, $S = S^\top$ by construction, and $S^2 = S$ since S is a projection. Therefore,

$$\begin{aligned} \|z^\perp\|^2 &= \|(S \otimes I_n)z\|^2 = z^\top (S \otimes I_n)^\top (S \otimes I_n)z \\ &= z^\top (S^\top \otimes I_n)(S \otimes I_n)z = z^\top (S^\top S \otimes I_n)z \\ &= z^\top (S^2 \otimes I_n)z = z^\top (S \otimes I_n)z \\ &= z^\top (VV^\top \otimes I_n)z = z^\top (V \otimes I_n)(V^\top \otimes I_n)z \\ &= \|(V^\top \otimes I_n)z\|^2, \end{aligned}$$

and the desired result follows. \blacksquare

Let $x^\circ \triangleq (V^\top \otimes I_n)x \in \mathbb{R}^{n(N-1)}$, and recall that consensus in $\{x_p\}_{p \in \mathcal{V}}$ is achieved whenever a solution of (14) converges to the agreement subspace defined by

$$\{x \in \mathbb{R}^{nN} : \forall p, q \in \mathcal{V} \ x_p = x_q\}. \quad (15)$$

Since the distance of an arbitrary configuration x to the agreement subspace in (15) is quantified by $\|x^\perp\|$ and $\|x^\perp\| = \|x^\circ\|$ by Lemma 2, $\|x^\circ\|$ is an alternative metric for consensus. Therefore, $x_p = x_q$ for all distinct $p, q \in \mathcal{V}$ if and only if $\|x^\circ\| = 0$.

The substitution of both identities in (1) and the ODE in (14) into the time derivative of x° yields⁵

$$\begin{aligned} \dot{x}^\circ &= ((I_{N-1} \otimes A) - (D \otimes BK_u H))x^\circ + (V^\top \otimes BK_u) \tilde{\eta} \\ &\quad + (V^\top \otimes BK_u)(1_{M^*}^\top \otimes I_{mN}) \tilde{\zeta}. \end{aligned} \quad (16)$$

Observe the matrix $(I_{N-1} \otimes A) - (D \otimes BK_u H)$ can be made stable through the selection of K_u , independent of the stability of A , provided (A, B) is controllable, (A, H) is observable, and $K_u H \neq 0_{d \times n}$ given [37, Lemma 2.2 & Theorem 2.6].⁶ Consider the block diagonal matrix $e \triangleq \text{diag}(e_1, e_2, \dots, e_N) \in \mathbb{R}^{N^2 \times N}$, where e_k denotes the k^{th} standard basis vector in \mathbb{R}^N . Substituting $L = LS$, (2), the output equation in (5), (11), and $x^\circ \triangleq (V^\top \otimes I_n)x$ into $\tilde{\eta}$ for every $p \in \mathcal{V}$ yields

$$\tilde{\eta} = \eta + Cx^\circ, \quad (17)$$

where $L_0 \triangleq \text{diag}(L[C_1], L[C_2], \dots, L[C_N]) \in \mathbb{R}^{N^2 \times N^2}$ and $C \triangleq (I_N \otimes H)(e^\top L_0 (I_N \otimes V) \otimes I_n) (1_N \otimes I_{n(N-1)}) \in \mathbb{R}^{mN \times n(N-1)}$.

⁵We remind the reader that, under Lemma 1, $L = VDV^\top$ with D being a diagonal positive definite matrix.

⁶Let $\lambda_1 > 0$ denote the smallest eigenvalue of D . Using a partial order on the space of positive semi definite matrices, one can show that $(I_{N-1} \otimes A) - (D \otimes BK_u H)$ is a stability matrix provided $A - \lambda_1 BK_u H$ is a stability matrix. Such a matrix K_u can be computed using [37, Theorem 2.6].

The substitution of the flow equation in (8) for each $p \in \mathcal{V}$, (16), and (17) into the time derivative of (17) yields

$$\begin{aligned} \dot{\tilde{\eta}} &= (\mathbf{C}((I_{N-1} \otimes A) - (\mathbf{D} \otimes BK_u H)) - K_\eta \mathbf{C})x^\circ \\ &\quad + (\mathbf{C}(\mathbf{V}^\top \otimes BK_u) + K_\eta)\tilde{\eta} \\ &\quad + \mathbf{C}(\mathbf{V}^\top \otimes BK_u)(1_{M^*}^\top \otimes I_{mN})\tilde{\zeta} \end{aligned} \quad (18)$$

with $K_\eta \triangleq \text{diag}(K_{\eta,1}, K_{\eta,2}, \dots, K_{\eta,N}) \in \mathbb{R}^{mN \times mN}$. Further, the substitution of $\mathbf{L} = \mathbf{L}\mathbf{S}$, (2), the output equation in (5), (12), and $x^\circ \triangleq (\mathbf{V}^\top \otimes I_n)x$ into $\tilde{\zeta}$ for every $p \in \mathcal{V}$ and $r \in [M^*]$ yields

$$\tilde{\zeta}_r = \zeta_r + \mathbf{l}_r x^\circ, \quad (19)$$

where $\mathbf{l}_r \triangleq (I_N \otimes H)(\mathbf{e}^\top (I_N \otimes \mathbf{L}[\mathcal{V}^r] \mathbf{V}) \otimes I_n)(1_N \otimes I_{n(N-1)}) \in \mathbb{R}^{mN \times n(N-1)}$. Substituting (19) for every $r \in [M^*]$ into $\tilde{\zeta}$ yields

$$\tilde{\zeta} = \zeta + \mathbf{l} x^\circ, \quad (20)$$

where $\mathbf{l} \triangleq \text{diag}(\mathbf{l}_1, \mathbf{l}_2, \dots, \mathbf{l}_{M^*})(1_{M^*} \otimes I_{n(N-1)})$. The substitution of the flow equation in (9) for every $p \in \mathcal{V}$ and $r \in [M^*]$, (16), and (20) into the time derivative of (20) yields

$$\begin{aligned} \dot{\tilde{\zeta}} &= (\mathbf{l}((I_{N-1} \otimes A) - (\mathbf{D} \otimes BK_u H)) - K_\zeta \mathbf{l})x^\circ \\ &\quad + \mathbf{l}(\mathbf{V}^\top \otimes BK_u)\tilde{\eta} \\ &\quad + (\mathbf{l}(\mathbf{V}^\top \otimes BK_u)(1_{M^*}^\top \otimes I_{mN}) + K_\zeta)\tilde{\zeta}, \end{aligned} \quad (21)$$

where $K_{\zeta,r} \triangleq \text{diag}(K_{\zeta,1r}, K_{\zeta,2r}, \dots, K_{\zeta,Nr}) \in \mathbb{R}^{mN \times mN}$ and $K_\zeta \triangleq \text{diag}(K_{\zeta,1}, K_{\zeta,2}, \dots, K_{\zeta,M^*}) \in \mathbb{R}^{mNM^* \times mNM^*}$.

Let $z \triangleq (x^\circ, \tilde{\eta}, \tilde{\zeta}) \in \mathbb{R}^{n(N-1) + mN + mNM^*}$. By leveraging the ODEs in (16), (18), and (21), a dynamical system can be developed for the variable z during flows, namely,

$$\dot{z} = \mathbf{F}z, \quad (22)$$

where

$$\mathbf{F} \triangleq \begin{bmatrix} \mathbf{F}_{11} & \mathbf{F}_{12} & \mathbf{F}_{13} \\ \mathbf{C}\mathbf{F}_{11} - K_\eta \mathbf{C} & \mathbf{C}\mathbf{F}_{12} + K_\eta & \mathbf{C}\mathbf{F}_{13} \\ \mathbf{l}\mathbf{F}_{11} - K_\zeta \mathbf{l} & \mathbf{l}\mathbf{F}_{12} & \mathbf{l}\mathbf{F}_{13} + K_\zeta \end{bmatrix},$$

$$\mathbf{F}_{11} \triangleq (I_{N-1} \otimes A) - (\mathbf{D} \otimes BK_u H)$$

$$\mathbf{F}_{12} \triangleq \mathbf{V}^\top \otimes BK_u, \quad \mathbf{F}_{13} \triangleq (\mathbf{V}^\top \otimes BK_u)(1_{M^*}^\top \otimes I_{mN}).$$

Let \mathcal{H} denote the closed-loop hybrid system for the ensemble. The state variable and state space of \mathcal{H} are denoted by $\xi \triangleq (z, \tau, \rho) \in \mathcal{X}$ and $\mathcal{X} \triangleq \mathbb{R}^{n(N-1)} \times \mathbb{R}^{mN} \times \mathbb{R}^{mNM^*} \times \mathcal{T} \times \mathcal{R}$, respectively. Observe $\mathcal{T} \triangleq [0, T_2^1] \times [0, T_2^2] \times \dots \times [0, T_2^N]$ and $\mathcal{R} \triangleq [0, T_4^1] \times [0, T_4^2] \times \dots \times [0, T_4^{M^*}]$. For every $p \in \mathcal{V}$ and $r \in [M^*]$, let

$$C_p \triangleq \{\xi \in \mathcal{X} : \tau_p \in [0, T_2^p]\}, \quad C^r \triangleq \{\xi \in \mathcal{X} : \rho_r \in [0, T_4^r]\}.$$

The flow set of \mathcal{H} is

$$C \triangleq \left(\bigcap_{p \in \mathcal{V}} C_p \right) \bigcap \left(\bigcap_{r \in [M^*]} C^r \right). \quad (23)$$

The differential equation governing the flows of \mathcal{H} is $\dot{\xi} = f(\xi)$, where the single-valued flow map $f: \mathcal{X} \rightarrow \mathcal{X}$ is

$$f(\xi) \triangleq \begin{bmatrix} \mathbf{F}z \\ -1_N \\ -1_{M^*} \end{bmatrix}. \quad (24)$$

The flow map in (24) follows from the substitution of the flow equation in (6) for each $p \in \mathcal{V}$, the flow equation in (7) for

each $r \in [M^*]$, and the dynamics of z in (22) into the time derivative of ξ . For each $p \in \mathcal{V}$ and $r \in [M^*]$, let

$$D_p \triangleq \{\xi \in \mathcal{X} : \tau_p = 0\}, \quad D^r \triangleq \{\xi \in \mathcal{X} : \rho_r = 0\}.$$

The jump set of \mathcal{H} is

$$D \triangleq \left(\bigcup_{p \in \mathcal{V}} D_p \right) \bigcup \left(\bigcup_{r \in [M^*]} D^r \right). \quad (25)$$

The differential inclusion governing the jumps of \mathcal{H} is $\xi^+ \in G(\xi)$, where the set-valued jump map $G: \mathcal{X} \rightrightarrows \mathcal{X}$ is

$$\begin{aligned} G(\xi) &\triangleq \{G_p(\xi) : \xi \in D_p \text{ for some } p \in \mathcal{V}\} \\ &\quad \cup \{G^r(\xi) : \xi \in D^r \text{ for some } r \in [M^*]\}, \\ G_p(\xi) &\triangleq \begin{bmatrix} x^\circ \\ [\tilde{\eta}_1^\top, \dots, \tilde{\eta}_{p-1}^\top, 0_m^\top, \tilde{\eta}_{p+1}^\top, \dots, \tilde{\eta}_N^\top]^\top \\ \tilde{\zeta} \\ [\tau_1, \dots, \tau_{p-1}, [T_1^p, T_2^p], \tau_{p+1}, \dots, \tau_N]^\top \\ \rho \end{bmatrix}, \\ G^r(\xi) &\triangleq \begin{bmatrix} x^\circ \\ \tilde{\eta} \\ [\tilde{\zeta}_1^\top, \dots, \tilde{\zeta}_{r-1}^\top, 0_{mN}^\top, \tilde{\zeta}_{r+1}^\top, \dots, \tilde{\zeta}_{M^*}^\top]^\top \\ \tau \\ [\rho_1, \dots, \rho_{r-1}, [T_3^r, T_4^r], \rho_{r+1}, \dots, \rho_{M^*}]^\top \end{bmatrix}. \end{aligned} \quad (26)$$

The jump map in (26) is derived by employing the following observations. Recall from (5) that, for each $p \in \mathcal{V}$, x_p evolves continuously, which implies that $x_p^+ = x_p$ at jumps. Therefore, $(x^\circ)^+ = x^\circ$ given $x^\circ = (\mathbf{V}^\top \otimes I_n)x$. The jump inclusion in (6) implies $\tau_p^+ \in [T_1^p, T_2^p]$ in response to a jump caused by $\tau_p = 0$, and $\tau_p^+ = \tau_p$ in response to a jump not caused by $\tau_p = 0$. Likewise, the jump inclusion in (7) implies $\rho_r^+ \in [T_3^r, T_4^r]$ in response to a jump caused by $\rho_r = 0$, and $\rho_r^+ = \rho_r$ in response to a jump not caused by $\rho_r = 0$. The jump equation in (8) and the definition in (11) imply $\tilde{\eta}_p^+ = 0_m$ whenever a jump occurs in response to $\tau_p = 0$, and $\tilde{\eta}_p^+ = \tilde{\eta}_p$ otherwise. Similarly, the jump equation in (9) and the definition in (12) imply $\tilde{\zeta}_{pr}^+ = 0_m$ for all $p \in \mathcal{V}^r$ whenever a jump occurs in response to $\rho_r = 0$, and $\tilde{\zeta}_{pr}^+ = \tilde{\zeta}_{pr}$ for all $p \in \mathcal{V}^r$ otherwise.

The solutions of the hybrid system \mathcal{H} with data (C, f, D, G) describe the behavior of the ensemble. Consequently, the MAS accomplishes consensus in the agents' states provided the set

$$\mathcal{A} \triangleq \{\xi \in \mathcal{X} : (x^\circ, \tilde{\eta}, \tilde{\zeta}) = (0_{n(N-1)}, 0_{mN}, 0_{mNM^*})\} \quad (27)$$

is GES. Therefore, the consensus problem can be transformed into a set stabilization problem for dynamical systems, which is the main focus of this work. In addition, since the set \mathcal{A} can be alternatively written as $\mathcal{A} = \{\xi \in \mathcal{X} : \|z\| = 0\}$, $\xi' \in \mathcal{A}$ if and only if $\xi' = (\mathbf{0}, \tau', \rho')$, $\tau' \in \mathcal{T}$, and $\rho' \in \mathcal{R}$, where $\mathbf{0}$ denotes a zero vector of appropriate dimension. As a result, for any $\xi \in \mathcal{X}$,

$$|\xi|_{\mathcal{A}} = \inf\{\|\xi - \xi'\| : \xi' \in \mathcal{A}\} = \|z\|. \quad (28)$$

Under the construction of \mathcal{H} , the flow set C and jump set D are closed. Additionally, the flow map f is continuous. The jump map G is outer semi-continuous and locally bounded. As a result, \mathcal{H} satisfies the hybrid basic conditions [32, Assumption 6.5], and [32, Theorem 6.8] implies \mathcal{H} is nominally well-posed.

V. STABILITY ANALYSIS

Before demonstrating \mathcal{A} is GES for the hybrid system \mathcal{H} , maximal solutions must first be shown to be complete so that the quantity $|\phi(t, j)|_{\mathcal{A}}$ is well-defined for arbitrarily large $t+j$. Two useful inequalities relating the continuous-time variable t and discrete-time variable j are also provided, which rely on the following constants:

$$\begin{aligned} T_{\min} &\triangleq \min\{T_1^p : p \in \mathcal{V}\} \cup \{T_3^r : r \in [M^*]\}, \\ T_{\max} &\triangleq \max\{T_2^p : p \in \mathcal{V}\} \cup \{T_4^r : r \in [M^*]\}. \end{aligned}$$

Lemma 3. For every maximal solution ϕ of the hybrid system \mathcal{H} with data (C, f, D, G) , the following items hold:

- 1) ϕ is complete.
- 2) The continuous-time t can be bounded by functions of the discrete-time j , i.e.,

$$\left(\frac{j}{N+M^*} - 1\right) T_{\min} \leq t \leq \frac{j}{N+M^*} T_{\max}. \quad (29)$$

for all $(t, j) \in \text{dom } \phi$. \triangle

Proof. See Appendix B. \blacksquare

To streamline the presentation of the main result, consider the following items. Let

$$\begin{aligned} T_2 &\triangleq (T_2^p)_{p \in \mathcal{V}} \in \mathbb{R}^N, \quad T_4 \triangleq (T_4^r)_{r \in [M^*]} \in \mathbb{R}^{M^*}, \\ T_2^{\max} &\triangleq \max\{T_2^p : p \in \mathcal{V}\} \in \mathbb{R}_{>0}. \end{aligned}$$

Let $\sigma \in \mathbb{R}_{>0}$ be a user-defined constant. Furthermore, let $P_1 \in \mathbb{R}^{n(N-1) \times n(N-1)}$, $P_{2,k} \in \mathbb{R}^{m \times m}$ for each $k \in \mathcal{V}$, and $P_{3,\ell} \in \mathbb{R}^{mN \times mN}$ for each $\ell \in [M^*]$ be user-defined, symmetric, and positive definite matrices. We can then use these matrices to define the following block diagonal matrices:

$$\begin{aligned} P_2(\tau) &\triangleq \text{diag}(P_{2,1} \exp(\sigma\tau_1), P_{2,2} \exp(\sigma\tau_2), \dots, \\ &\quad P_{2,N} \exp(\sigma\tau_N)) \in \mathbb{R}^{mN \times mN}, \\ P_3(\rho) &\triangleq \text{diag}(P_{3,1} \exp(\sigma\rho_1), P_{3,2} \exp(\sigma\rho_2), \dots, \\ &\quad P_{3,M^*} \exp(\sigma\rho_{M^*})) \in \mathbb{R}^{mNM^* \times mNM^*}, \\ P(\tau, \rho) &\triangleq \text{diag}(P_1, P_2(\tau), P_3(\rho)). \end{aligned} \quad (30)$$

Moreover, let

$$\begin{aligned} M(\tau, \rho) &\triangleq F^\top P(\tau, \rho) + P(\tau, \rho)F + \dot{P}(\tau, \rho), \\ \mu &\triangleq -\sup\{\lambda_{\max}(M(\tau, \rho)) : (\tau, \rho) \in \mathcal{T} \times \mathcal{R}\}, \\ \alpha_1 &\triangleq \lambda_{\min}(P(0_N, 0_{M^*})), \quad \alpha_2 \triangleq \lambda_{\max}(P(T_2, T_4)), \\ \dot{P}(\tau, \rho) &= -\sigma \text{diag}(0_{n(N-1) \times n(N-1)}, P_2(\tau), P_3(\rho)). \end{aligned} \quad (31)$$

By definition, the matrix M is symmetric. If M satisfies $M < \mathbf{0}$ for all $(\tau, \rho) \in \mathcal{T} \times \mathcal{R}$, then the constant μ is positive. Further, $\alpha_1 \in \mathbb{R}_{>0}$ and $\alpha_2 \in \mathbb{R}_{>0}$ since $P(\tau, \rho)$ is positive definite.

Theorem 1. If there exist timer parameters $0 < T_1^p \leq T_2^p$ for every $p \in \mathcal{V}$ and $0 < T_3^r \leq T_4^r$ for every $r \in [M^*]$, a constant σ , controller matrix K_u , estimator matrices $K_{\eta,p}$ for each $p \in \mathcal{V}$, estimator matrices $K_{\zeta,pr}$ for every $(p, r) \in \mathcal{V} \times [M^*]$, and symmetric, positive definite matrices P_1 , $P_2(\tau)$, and $P_3(\rho)$ that satisfy the inequality $M(\tau, \rho) < \mathbf{0}$ for all $(\tau, \rho) \in \mathcal{T} \times \mathcal{R}$, then the set \mathcal{A} in (27) is GES for the hybrid system \mathcal{H} with

data (C, f, D, G) . In particular, for every maximal solution ϕ of \mathcal{H} ,

$$|\phi(t, j)|_{\mathcal{A}} \leq \kappa \exp(-\alpha(t+j)) |\phi(0, 0)| \quad (32)$$

for all $(t, j) \in \text{dom } \phi$, where, for some constant $\varepsilon \in (0, 1)$,

$$\begin{aligned} \kappa &\triangleq \sqrt{\frac{\alpha_2}{\alpha_1} \exp\left(\frac{(1-\varepsilon)\mu T_{\min}}{\alpha_2}\right)} \in \mathbb{R}_{>0}, \\ \alpha &\triangleq \frac{1}{2} \min\left\{\frac{\varepsilon\mu}{\alpha_2}, \frac{(1-\varepsilon)\mu T_{\min}}{\alpha_2(N+M^*)}\right\} \in \mathbb{R}_{>0}, \end{aligned}$$

and $\mu \in \mathbb{R}_{>0}$. Furthermore, the controllers $\{u_p(\phi(t, j))\}_{p \in \mathcal{V}}$ in (10) are bounded for all $(t, j) \in \text{dom } \phi$. \triangle

Proof. Consider the Lyapunov function candidate

$$V : \mathcal{X} \rightarrow \mathbb{R}_{\geq 0} : \xi \mapsto z^\top P(\tau, \rho)z. \quad (33)$$

Using $|\xi|_{\mathcal{A}} = \|z\|$ given (28) and the definitions of α_1 and α_2 in (31), the Lyapunov function candidate $V(\xi)$ can be bounded as

$$\alpha_1 |\xi|_{\mathcal{A}}^2 \leq V(\xi) \leq \alpha_2 |\xi|_{\mathcal{A}}^2. \quad (34)$$

When $\xi \in C$, the change in $V(\xi)$ is computed using $\dot{V}(\xi) = \langle \nabla V(\xi), f(\xi) \rangle$ given that $V(\xi)$ is continuously differentiable in ξ . Substituting the flow map in (24) into the time derivative of (33) yields

$$\begin{aligned} \dot{V}(\xi) &= 2z^\top P(\tau, \rho)Fz + z^\top \dot{P}(\tau, \rho)z \\ &= z^\top (F^\top P(\tau, \rho) + P(\tau, \rho)F + \dot{P}(\tau, \rho))z \\ &= z^\top M(\tau, \rho)z. \end{aligned} \quad (35)$$

Since $M(\tau, \rho)$ is negative definite for all $(\tau, \rho) \in \mathcal{T} \times \mathcal{R}$ by the hypothesis, the constant μ is positive. Using the definition of μ in (31), $|\xi|_{\mathcal{A}} = \|z\|$, and $V(\xi) \leq \alpha_2 |\xi|_{\mathcal{A}}^2$ from (34), one can bound (35) as

$$\dot{V}(\xi) \leq -\mu \|z\|^2 = -\mu |\xi|_{\mathcal{A}}^2 \leq -\frac{\mu}{\alpha_2} V(\xi). \quad (36)$$

When $\xi \in D$ and $g \in G(\xi)$, the change in $V(\xi)$ is computed using $\Delta V(\xi) = V(g) - V(\xi)$. Suppose $\tau_q = 0$ and $\rho_s = 0$ for some $q \in \mathcal{V}$ and $s \in [M^*]$ without loss of generality. Hence, the jump map in (26) implies that⁷

$$\begin{aligned} \Delta V(\xi) &= (z^+)^{\top} P(\tau^+, \rho^+)(z^+) - z^{\top} P(\tau, \rho)z \\ &= -\tilde{\eta}_q^{\top} P_{2,q} \tilde{\eta}_q - \tilde{\zeta}_s^{\top} P_{3,s} \tilde{\zeta}_s \leq 0 \end{aligned} \quad (37)$$

since $(x^\circ)^+ = x^\circ$ after any jump, $\tilde{\eta}_q^+ = 0_m$ and $\tilde{\eta}_p^+ = \tilde{\eta}_p$ for all $p \in \mathcal{V} \setminus \{q\}$ in response to a jump caused by $\tau_q = 0$, and $\tilde{\zeta}_s^+ = 0_{mN}$ and $\tilde{\zeta}_r^+ = \tilde{\zeta}_r$ for all $r \in [M^*] \setminus \{s\}$ in response to a jump caused by $\rho_s = 0$.

Next, fix a maximal solution ϕ of \mathcal{H} , select $(t, j) \in \text{dom } \phi$, and let $0 = t_0 \leq t_1 \leq \dots \leq t_j \leq t$ satisfy

$$\text{dom } \phi \cap ([0, t_j] \times \{0, 1, \dots, j-1\}) = \bigcup_{k=1}^j ([t_{k-1}, t_k] \times \{k-1\}).$$

⁷The result in (37) also follows if $\tau_q = 0$, $\rho_s = 0$, or any combination of timers take on a value of 0.

For every $k \in \{1, 2, \dots, j\}$ and for almost all $h \in [t_{k-1}, t_k]$, $\phi(h, k-1) \in \mathcal{C}$. Furthermore, for every $k \in \{1, 2, \dots, j\}$ and for almost all $h \in [t_{k-1}, t_k]$, (36) implies

$$\frac{d}{dh}V(\phi(h, k-1)) \leq -\frac{\mu}{\alpha_2}V(\phi(h, k-1)). \quad (38)$$

Integrating both sides of (38) yields

$$V(\phi(t_k, k-1)) \leq \exp\left(-\frac{\mu}{\alpha_2}(t_k - t_{k-1})\right)V(\phi(t_{k-1}, k-1)) \quad (39)$$

for every $k \in \{1, 2, \dots, j\}$. Similarly, for each $k \in \{1, 2, \dots, j\}$ with $\phi(t_k, k-1) \in D$, (37) implies

$$V(\phi(t_k, k)) \leq V(\phi(t_k, k-1)). \quad (40)$$

By inductively stitching the inequalities in (39) and (40) along the maximal solution ϕ , it follows that

$$V(\phi(t, j)) \leq \exp\left(-\frac{\mu}{\alpha_2}t\right)V(\phi(0, 0)). \quad (41)$$

Using the left inequality in (29) and the identity $t = \varepsilon t + (1 - \varepsilon)t$, one can derive

$$-\frac{\mu}{\alpha_2}t \leq -\min\left\{\frac{\varepsilon\mu}{\alpha_2}, \frac{(1-\varepsilon)\mu T_{\min}}{\alpha_2(N+M^*)}\right\}(t+j) + \frac{(1-\varepsilon)\mu T_{\min}}{\alpha_2}, \quad (42)$$

which, when substituted into (41), yields

$$V(\phi(t, j)) \leq \exp\left(-\min\left\{\frac{\varepsilon\mu}{\alpha_2}, \frac{(1-\varepsilon)\mu T_{\min}}{\alpha_2(N+M^*)}\right\}(t+j)\right) \cdot \exp\left(\frac{(1-\varepsilon)\mu T_{\min}}{\alpha_2}\right)V(\phi(0, 0)). \quad (43)$$

The application of the inequalities in (34) on (43) yields

$$|\phi(t, j)|_{\mathcal{A}}^2 \leq \frac{\alpha_2}{\alpha_1} \exp\left(-\min\left\{\frac{\varepsilon\mu}{\alpha_2}, \frac{(1-\varepsilon)\mu T_{\min}}{\alpha_2(N+M^*)}\right\}(t+j)\right) \cdot \exp\left(\frac{(1-\varepsilon)\mu T_{\min}}{\alpha_2}\right)|\phi(0, 0)|_{\mathcal{A}}^2, \quad (44)$$

which leads to the desired bound in (32). Therefore, the set \mathcal{A} is GES since every maximal solution ϕ of \mathcal{H} is complete by Lemma 3 and $|\phi(t, j)|_{\mathcal{A}}$ is bounded according to (32), with $\kappa, \alpha > 0$, for all $(t, j) \in \text{dom } \phi$.

Using (33) and (43), one can conclude that $z = z(\phi(t, j))$ is bounded for all $(t, j) \in \text{dom } \phi$. Recall $(V^\top \otimes I_n)$ is full rank. Thus, $z = (x^\circ, \tilde{\eta}, \tilde{\zeta})$ implies $x_p, \tilde{\eta}_p$, and $\tilde{\zeta}_{pr}$ are bounded for all $p \in \mathcal{V}$ and all $r \in [M^*]$. Using the output equation in (5), x_p being bounded implies y_p is bounded for all $p \in \mathcal{V}$. Hence, u_p is bounded for all $p \in \mathcal{V}$ given (8)–(10) and the bounded flow intervals of \mathcal{H} , i.e., $t_{j+1} - t_j \leq T_{\max}$ for all $(t_j)_{j=0}^\infty$. ■

With respect to Theorem 1, the global exponential stability of \mathcal{A} for \mathcal{H} requires $M(\tau, \rho) < \mathbf{0}$ to hold for all $(\tau, \rho) \in \mathcal{T} \times \mathcal{R}$. In other words, $M(\tau, \rho) < \mathbf{0}$ must hold for an infinite number of points, which cannot be exhaustively verified in practice. Hence, the following result is motivated.

For each $p \in \mathcal{V}$ and $r \in [M^*]$, let $\gamma_p: [0, T_2^p] \rightarrow [0, 1]$ and $\gamma^r: [0, T_4^r] \rightarrow [0, 1]$, such that

$$\begin{aligned} \gamma_p(w) &\triangleq \frac{\exp(\sigma w) - \exp(\sigma T_2^p)}{1 - \exp(\sigma T_2^p)}, \\ \gamma^r(w) &\triangleq \frac{\exp(\sigma w) - \exp(\sigma T_4^r)}{1 - \exp(\sigma T_4^r)}. \end{aligned} \quad (45)$$

Also, let $\epsilon \in [0, 1]$ and $\theta \triangleq (\epsilon, \tau, \rho) \in \Theta$, where $\Theta \triangleq [0, 1] \times \mathcal{T} \times \mathcal{R}$. We can then construct the following block diagonal matrices:

$$\begin{aligned} R_2(\tau) &\triangleq \text{diag}(\gamma_1(\tau_1), \gamma_2(\tau_2), \dots, \gamma_N(\tau_N)) \otimes I_m, \\ R_3(\rho) &\triangleq \text{diag}(\gamma^1(\rho_1), \gamma^2(\rho_2), \dots, \gamma^{M^*}(\rho_{M^*})) \otimes I_{mN}, \\ R(\theta) &\triangleq \text{diag}(\epsilon I_{n(N-1)}, R_2(\tau), R_3(\rho)), \end{aligned} \quad (46)$$

where $R_2(\tau) \in \mathbb{R}^{mN \times mN}$ and $R_3(\rho) \in \mathbb{R}^{mNM^* \times mNM^*}$.

Corollary 1. If there exist timer parameters $0 < T_1^p \leq T_2^p$ for each agent $p \in \mathcal{V}$ and $0 < T_3^r \leq T_4^r$ for each $r \in [M^*]$, a constant σ , controller matrix K_u , estimator matrices $K_{\eta, p}$ for each $p \in \mathcal{V}$, estimator matrices $K_{\zeta, pr}$ for every $(p, r) \in \mathcal{V} \times [M^*]$, and symmetric, positive definite matrices $P_1, P_{2, p}$ for every $p \in \mathcal{V}$, and $P_{3, r}$ for every $r \in [M^*]$ that satisfy $M(0_N, 0_{M^*}) < \mathbf{0}$ and $M(T_2, T_4) < \mathbf{0}$, then $M(\tau, \rho) < \mathbf{0}$ for all $(\tau, \rho) \in \mathcal{T} \times \mathcal{R}$. \triangle

Proof. For all $p \in \mathcal{V}$ and $r \in [M^*]$, the functions in (45) can be written as

$$\begin{aligned} \exp(\sigma \tau_p) &= \gamma_p(\tau_p) + (1 - \gamma_p(\tau_p)) \exp(\sigma T_2^p), \\ \exp(\sigma \rho_r) &= \gamma^r(\rho_r) + (1 - \gamma^r(\rho_r)) \exp(\sigma T_4^r). \end{aligned} \quad (47)$$

Using the equations in (47) and the definitions of $P(\tau, \rho)$ and $R(\theta)$, one can derive

$$\begin{aligned} P(\tau, \rho) &= R(\theta)P(0_N, 0_{M^*}) + (I_\varrho - R(\theta))P(T_2, T_4), \\ \dot{P}(\tau, \rho) &= R(\theta)\dot{P}(0_N, 0_{M^*}) + (I_\varrho - R(\theta))\dot{P}(T_2, T_4), \end{aligned} \quad (48)$$

where $\varrho \triangleq n(N-1) + mN + mNM^*$. Let v be an arbitrary real-valued vector such that the quadratic form $v^\top M(\tau, \rho)v$ is well-defined. Using the definition of M in (31), one can obtain

$$v^\top M(\tau, \rho)v = 2v^\top P(\tau, \rho)Fv + v^\top \dot{P}(\tau, \rho)v. \quad (49)$$

The substitution of (48) into (49) yields

$$\begin{aligned} v^\top M(\tau, \rho)v &= v^\top R(\theta)(2P(0_N, 0_{M^*})F + \dot{P}(0_N, 0_{M^*}))v \\ &\quad + v^\top (I_\varrho - R(\theta))(2P(T_2, T_4)F + \dot{P}(T_2, T_4))v. \end{aligned} \quad (50)$$

Since the matrices $P(\tau, \rho)$, $\dot{P}(\tau, \rho)$, and $R(\theta)$ are symmetric, (50) can be simplified to

$$\begin{aligned} v^\top M(\tau, \rho)v &= v^\top R(\theta)M(0_N, 0_{M^*})R(\theta)v \\ &\quad + v^\top (I_\varrho - R(\theta))M(T_2, T_4)(I_\varrho - R(\theta))v. \end{aligned} \quad (51)$$

Although the matrices $R(\theta)$ and $I_\varrho - R(\theta)$ are positive semi-definite for all $\theta \in \Theta$, $R(\theta)v$ and $(I_\varrho - R(\theta))v$ cannot be zero simultaneously for any $\theta \in \Theta$ and $v \neq \mathbf{0}$. Thus, for all $v \neq \mathbf{0}$, $M(0_N, 0_{M^*}) < \mathbf{0}$, $M(T_2, T_4) < \mathbf{0}$, and the equality in (51) imply $M(\tau, \rho) < \mathbf{0}$ for all $(\tau, \rho) \in \mathcal{T} \times \mathcal{R}$. ■

Corollary 1 provides a convenient method for validating the sufficient condition of Theorem 1. Specifically, Corollary 1

only requires the checking of two matrix inequalities, namely, $M(0_N, 0_{M^*}) < \mathbf{0}$ and $M(T_2, T_4) < \mathbf{0}$, to ensure $M(\tau, \rho) < \mathbf{0}$ holds for all $(\tau, \rho) \in \mathcal{T} \times \mathcal{R}$.

VI. ROBUSTNESS

In this section, we briefly discuss the robustness properties of the set \mathcal{A} for the hybrid system \mathcal{H} . Since \mathcal{H} is nominally well-posed and the set \mathcal{A} is compact and GES for \mathcal{H} , standard arguments can be used to show that \mathcal{A} is robust to vanishing perturbations for \mathcal{H} (for example, see [32, Section 7.3] and [38, Section 3.5.1]). The reader is referred to [32, Chapter 7] for results showcasing the robustness of \mathcal{A} for \mathcal{H} , which is due to the structure of \mathcal{A} and \mathcal{H} and the exponential stability of \mathcal{A} . For the remainder of this section, we examine the robustness of \mathcal{A} to non-vanishing measurement noise injected via a modified jump map of \mathcal{H} .

The evolution of the variable η_p under the hybrid dynamics in (8) is ideal because the output information in $\{y_q\}_{q \in \mathcal{N}_p \cap \mathcal{C}_p}$ is measured exactly and without corrupting noise when determined by the timer τ_p . An analogous comment follows for ζ_{pr} . Nevertheless, in practice, none-vanishing measurement noise will be present, and its effect on the GES result in Theorem 1 should be explored to determine the utility of the proposed consensus strategy. In light of this need, consider the following modifications of (8) and (9):

$$\begin{aligned} \dot{\eta}_p &= K_{\eta,p} \eta_p, & \tau_p &\in [0, T_2^p] \\ \eta_p^+ &= \sum_{q \in \mathcal{N}_p \cap \mathcal{C}_p} (y_q - y_p) + \delta_p, & \tau_p &= 0 \end{aligned} \quad (52)$$

and

$$\begin{aligned} \dot{\zeta}_{pr} &= K_{\zeta,pr} \zeta_{pr}, & \rho_r &\in [0, T_4^r] \\ \zeta_{pr}^+ &= \sum_{q \in \mathcal{N}_p \cap \mathcal{V}^r} (y_q - y_p) + \delta_{pr}, & \rho_r &= 0, \end{aligned} \quad (53)$$

where $\delta_p, \delta_{pr} \in \mathbb{R}^m$ model non-vanishing measurement noise. Typically, measurement noise is additively injected, e.g., $y_p + \delta_p$, which would imply $\eta_p^+ = \sum_{q \in \mathcal{N}_p \cap \mathcal{C}_p} (y_q - y_p + \delta_q - \delta_p)$. Nevertheless, we consider the lumped perturbation δ_p instead of $\sum_{q \in \mathcal{N}_p \cap \mathcal{C}_p} (\delta_q - \delta_p)$ for convenience. A similar statement follows for δ_{pr} . Nearly all other components of \mathcal{H} , that is, the flow equations of $x^\circ, \tilde{\eta}, \tilde{\zeta}, \tau$, and ρ , the definitions in (11) and (12), and the jump equations/inclusions of x°, τ , and ρ , will remain unchanged. Yet, under the jump equations of (52) and (53), the jump equations of $\tilde{\eta}_p$ and $\tilde{\zeta}_{pr}$ do change.

The definition in (11) and jump equation in (52) imply $\tilde{\eta}_p^+ = \delta_p$ whenever a jump occurs in response to $\tau_p = 0$, and $\tilde{\eta}_p^+ = \tilde{\eta}_p$ otherwise. Likewise, (12) and the jump equation in (53) imply $\tilde{\zeta}_{pr}^+ = \delta_{pr}$ for all $p \in \mathcal{V}^r$ whenever a jump occurs in response to $\rho_r = 0$, and $\tilde{\zeta}_{pr}^+ = \tilde{\zeta}_{pr}$ for all $p \in \mathcal{V}^r$ otherwise. With these observations in place, we construct a modification of \mathcal{H} .

Let $\mathcal{D} \subseteq \mathbb{R}^{mN} \times \mathbb{R}^{mNM^*}$, and consider the hybrid system \mathcal{K} with flow set $\tilde{C} \triangleq C \times \mathcal{D}$, jump set $\tilde{D} \triangleq D \times \mathcal{D}$, single-valued flow map $\tilde{f}: \mathcal{X} \times \mathcal{D} \rightarrow \mathcal{X}$ by $\tilde{f}(\xi, \delta) = f(\xi)$, and set-valued jump map $\tilde{G}: \mathcal{X} \times \mathcal{D} \rightrightarrows \mathcal{X}$. Furthermore, let $\delta^r \triangleq (\delta_{pr})_{p \in \mathcal{V}}$, $\delta \triangleq ((\delta_p)_{p \in \mathcal{V}}, (\delta^r)_{r \in [M^*]}) \in \mathcal{D}$,

$$\begin{aligned} \tilde{G}(\xi, \delta) &\triangleq \{ \tilde{G}_p(\xi, \delta) : (\xi, \delta) \in D_p \times \mathcal{D} \text{ for } p \in \mathcal{V} \} \\ &\cup \{ \tilde{G}^r(\xi, \delta) : (\xi, \delta) \in D^r \times \mathcal{D} \text{ for } r \in [M^*] \}, \end{aligned}$$

$$\begin{aligned} \tilde{G}_p(\xi, \delta) &\triangleq \begin{bmatrix} x^\circ \\ [\tilde{\eta}_1^\top, \dots, \tilde{\eta}_{p-1}^\top, \delta_p^\top, \tilde{\eta}_{p+1}^\top, \dots, \tilde{\eta}_N^\top]^\top \\ \tilde{\zeta} \\ [\tau_1, \dots, \tau_{p-1}, [T_1^p, T_2^p], \tau_{p+1}, \dots, \tau_N]^\top \\ \rho \end{bmatrix}, \\ \tilde{G}^r(\xi, \delta) &\triangleq \begin{bmatrix} x^\circ \\ \tilde{\eta} \\ [\tilde{\zeta}_1^\top, \dots, \tilde{\zeta}_{r-1}^\top, (\tilde{\zeta}_{pr}^+)^\top_{p \in \mathcal{V}}, \tilde{\zeta}_{r+1}^\top, \dots, \tilde{\zeta}_{M^*}^\top]^\top \\ \tau \\ [\rho_1, \dots, \rho_{r-1}, [T_3^r, T_4^r], \rho_{r+1}, \dots, \rho_{M^*}]^\top \end{bmatrix}, \\ \tilde{\zeta}_{pr}^+ &= \begin{cases} \delta_{pr}, & p \in \mathcal{V}^r \\ 0_m, & p \notin \mathcal{V}^r. \end{cases} \end{aligned} \quad (54)$$

Theorem 2. If there exist timer parameters $0 < T_1^p \leq T_2^p$ for every $p \in \mathcal{V}$ and $0 < T_3^r \leq T_4^r$ for every $r \in [M^*]$, a constant σ , controller matrix K_u , estimator matrices $K_{\eta,p}$ for each $p \in \mathcal{V}$, estimator matrices $K_{\zeta,pr}$ for every $(p, r) \in \mathcal{V} \times [M^*]$, and symmetric, positive definite matrices $P_1, P_2(\tau)$, and $P_3(\rho)$ that satisfy the inequality $M(\tau, \rho) < \mathbf{0}$ for all $(\tau, \rho) \in \mathcal{T} \times \mathcal{R}$, then the set \mathcal{A} in (27) is ISS for the hybrid system \mathcal{K} with data $(\tilde{C}, \tilde{f}, \tilde{D}, \tilde{G})$. In particular, for every solution pair (ϕ, δ) of \mathcal{K} ,

$$|\phi(t, j)|_{\mathcal{A}} \leq \max\{2\kappa \exp(-\alpha(t+j))|\phi(0, 0)|, 2\kappa_2|\delta|_\infty\}, \quad (55)$$

where $N^* \triangleq N + M^* \in \mathbb{Z}_{>0}$,⁸

$$\begin{aligned} p_{\max} &\triangleq \lambda_{\max}(\text{diag}(P_2(T_2), P_3(T_4))) \in \mathbb{R}_{>0}, \text{ and} \\ \kappa_2 &\triangleq \sqrt{\frac{p_{\max} N^* (2 - \exp(-\mu T_{\min}/\alpha_2))}{\alpha_1 (1 - \exp(-\mu T_{\min}/\alpha_2))}} \in \mathbb{R}_{>0}. \end{aligned}$$

Recall, κ and α are defined in Theorem 1. \triangle

Proof. Consider the Lyapunov function candidate in (33) and the hybrid system \mathcal{K} . When $(\xi, \delta) \in \tilde{C}$, the change in $V(\xi)$ is captured by $\dot{V}(\xi) = z^\top M(\tau, \rho)z$. Since $M(\tau, \rho)$ is negative definite for all $(\tau, \rho) \in \mathcal{T} \times \mathcal{R}$, the time derivative of (33) can be bounded as in (36) using the same argument as in the proof of Theorem 1.

When $(\xi, \delta) \in \tilde{D}$, the change in $V(\xi)$ is given by $\Delta V(\xi) = V(g) - V(\xi)$ where $g \in \tilde{G}(\xi, \delta)$. Suppose $\tau_q = 0$ and $\rho_s = 0$ for some $q \in \mathcal{V}$ and $s \in [M^*]$. It then follows that

$$\begin{aligned} \Delta V(\xi) &= (z^+)^{\top} P(\tau^+, \rho^+)(z^+) - z^{\top} P(\tau, \rho)z \\ &= \delta_q^{\top} P_{2,q} \exp(\sigma \tau_q^+) \delta_q + (\delta^s)^{\top} P_{3,s} \exp(\sigma \rho_s^+) \delta^s \\ &\quad - \tilde{\eta}_q^{\top} P_{2,q} \tilde{\eta}_q - \tilde{\zeta}_s^{\top} P_{3,s} \tilde{\zeta}_s \\ &\leq \delta_q^{\top} P_{2,q} \exp(\sigma T_2^q) \delta_q + (\delta^s)^{\top} P_{3,s} \exp(\sigma T_4^s) \delta^s. \end{aligned} \quad (56)$$

From (56), we can see that the change in $V(\xi)$ may be positive after a jump, which would cause the value of V to increase. In

⁸The matrices $P_2(\tau)$ and $P_3(\rho)$ are defined in (30), while the definitions of the constant vectors T_2 and T_4 are located above (30).

the worst-case scenario, i.e., when all agents and inter-clusters experience a simultaneous jump, one has that

$$\begin{aligned} \Delta V(\xi) &\leq ((\delta_p)_{p \in \mathcal{V}})^\top P_2(T_2)(\delta_p)_{p \in \mathcal{V}} \\ &\quad + ((\delta^r)_{r \in [M^*]})^\top P_3(T_4)(\delta^r)_{r \in [M^*]} \\ &\leq p_{\max} |\delta|_\infty^2. \end{aligned} \quad (57)$$

Substituting $\Delta V(\xi) = V(g) - V(\xi)$ into (57) yields

$$V(g) \leq p_{\max} |\delta|_\infty^2 + V(\xi). \quad (58)$$

Next, fix a solution pair (ϕ, δ) for the hybrid system \mathcal{K} , select $(t, j) \in \text{dom}(\phi, \delta)$, and let $0 = t_0 \leq t_1 \leq \dots \leq t_j \leq t$ satisfy

$$\begin{aligned} &\text{dom}(\phi, \delta) \cap ([0, t_j] \times \{0, 1, \dots, j-1\}) \\ &= \bigcup_{k=1}^j ([t_{k-1}, t_k] \times \{k-1\}). \end{aligned}$$

Using a similar argument to that in the proof of Theorem 1 with $(\phi(h, k-1), \delta(h, k-1)) \in \tilde{C}$ for almost all $h \in [t_{k-1}, t_k]$ and each $k \in \{1, 2, \dots, j\}$, one can show that

$$V(\phi(t_k, k-1)) \leq \exp\left(-\frac{\mu}{\alpha_2}(t_k - t_{k-1})\right) V(\phi(t_{k-1}, k-1)). \quad (59)$$

For each $(\phi(t_k, k-1), \delta((t_k, k-1))) \in \tilde{D}$ and $k \in \{1, 2, \dots, j\}$, the inequality in (58) implies

$$V(\phi(t_k, k)) \leq p_{\max} |\delta|_\infty^2 + V(\phi(t_k, k-1)). \quad (60)$$

One can then inductively stitch (59) and (60) along the solution ϕ to obtain

$$\begin{aligned} V(\phi(t, j)) &\leq \exp\left(-\frac{\mu}{\alpha_2}t\right) V(\phi(0, 0)) \\ &\quad + p_{\max} |\delta|_\infty^2 \sum_{s=1}^j \exp\left(-\frac{\mu}{\alpha_2}(t_j - t_s)\right), \end{aligned} \quad (61)$$

where we used the fact that $t_j \leq t$ and $V(\xi)$ is non-increasing during flows. A bound for the series in (61) is derived next.

Let $j^* \triangleq \lfloor j/N^* \rfloor \in \mathbb{Z}_{\geq 0}$. Note $j^*N^* \leq j$ and $j - j^*N^* \leq N^*$. The summation in (61) can be rewritten as

$$\begin{aligned} \sum_{s=1}^j \exp\left(-\frac{\mu}{\alpha_2}(t_j - t_s)\right) &= \sum_{s=0}^{j^*-1} \sum_{k=1}^{N^*} \exp\left(-\frac{\mu}{\alpha_2}(t_j - t_{sN^*+k})\right) \\ &\quad + \sum_{s=j^*N^*+1}^j \exp\left(-\frac{\mu}{\alpha_2}(t_j - t_s)\right). \end{aligned} \quad (62)$$

Note that $\exp(-\frac{\mu}{\alpha_2}(t_j - t_{sN^*+k})) \leq \exp(-\frac{\mu}{\alpha_2}(t_j - t_{(s+1)N^*}))$ for each $k \in [N^*]$ since $t_{sN^*+1} \leq t_{sN^*+2} \leq \dots \leq t_{(s+1)N^*} \leq t_j$. Therefore,

$$\sum_{k=1}^{N^*} \exp\left(-\frac{\mu}{\alpha_2}(t_j - t_{sN^*+k})\right) \leq N^* \exp\left(-\frac{\mu}{\alpha_2}t_j^{s+1}\right), \quad (63)$$

where $t_j^{s+1} \triangleq t_j - t_{(s+1)N^*}$. Furthermore, since $\exp(-\frac{\mu}{\alpha_2}(t_j - t_s)) \leq 1$ provided $t_j - t_s \geq 0$ and $t_{j^*N^*+1} \leq t_{j^*N^*+2} \leq \dots \leq t_j$, one has that

$$\sum_{s=j^*N^*+1}^j \exp\left(-\frac{\mu}{\alpha_2}(t_j - t_s)\right) \leq j - j^*N^* \leq N^*. \quad (64)$$

Given (63) and (64), the series in (62) can be bounded as

$$\sum_{s=1}^j \exp\left(-\frac{\mu}{\alpha_2}(t_j - t_s)\right) \leq \sum_{s=0}^{j^*-1} N^* \exp\left(-\frac{\mu}{\alpha_2}t_j^{s+1}\right) + N^*. \quad (65)$$

With respect to the right-hand side of (62), the outer summation in the left term describes jumps that occur simultaneously between all agents and inter-clusters; the right term describes individual jumps taken by agents or inter-clusters. In the case of simultaneous jumps, one can show that $T_{\min} \leq t_{(s+1)N^*} - t_{sN^*} \leq T_{\max}$ for $s = 0, 1, \dots, j^*-1$. In addition, one can show $t_{j^*N^*} - t_{(s+1)N^*} \geq (j^* - (s+1))T_{\min}$ for $s = 0, 1, \dots, j^*-1$. Leveraging $t_j \geq t_{j^*N^*}$, $t_{j^*N^*} - t_{(s+1)N^*} \geq (j^* - (s+1))T_{\min}$, and (65), it follows that

$$\sum_{s=1}^j \exp\left(-\frac{\mu}{\alpha_2}(t_j - t_s)\right) \leq \sum_{s=0}^{j^*-1} N^* \exp\left(-s\frac{\mu}{\alpha_2}T_{\min}\right) + N^*. \quad (66)$$

Note $j^* \rightarrow \infty$ as $j \rightarrow \infty$ since $j^* = \lfloor j/N^* \rfloor$. Moreover, since $\exp(-\mu T_{\min}/\alpha_2) \in (0, 1)$, the corresponding geometric series converges, that is,

$$\begin{aligned} \sum_{s=0}^{\infty} N^* \exp\left(-s\frac{\mu}{\alpha_2}T_{\min}\right) &= N^* \sum_{s=0}^{\infty} \exp\left(-\frac{\mu}{\alpha_2}T_{\min}\right)^s \\ &= \frac{N^*}{1 - \exp(-\mu T_{\min}/\alpha_2)}. \end{aligned} \quad (67)$$

Thus, (66) and (67) imply

$$\sum_{s=1}^j \exp\left(-\frac{\mu}{\alpha_2}(t_j - t_s)\right) \leq \frac{N^*(2 - \exp(-\mu T_{\min}/\alpha_2))}{1 - \exp(-\mu T_{\min}/\alpha_2)}. \quad (68)$$

The substitution of (68) into (61) yields

$$\begin{aligned} V(\phi(t, j)) &\leq \exp\left(-\frac{\mu}{\alpha_2}t\right) V(\phi(0, 0)) \\ &\quad + p_{\max} |\delta|_\infty^2 N^* \frac{2 - \exp(-\mu T_{\min}/\alpha_2)}{1 - \exp(-\mu T_{\min}/\alpha_2)}. \end{aligned} \quad (69)$$

Upon substituting (42) into (69) and using the bounds in (34), the desired result in (55) follows. \blacksquare

VII. SIMULATION EXAMPLE & DISCUSSION

To confirm the theoretical results, we consider a rendezvous application for a MAS of identical marine crafts maneuvering on a common plane. The kinematics of agent p are

$$\dot{c}_{1,p} = v_p \cos(\theta_p), \quad \dot{c}_{2,p} = v_p \sin(\theta_p), \quad \dot{\theta}_p = \omega_p. \quad (70)$$

For each $p \in \mathcal{V}$, suppose the center of mass (CM) of marine craft p is fixed. The position of the CM of agent p is denoted by $c_p \triangleq (c_{1,p}, c_{2,p}) \in \mathbb{R}^2$ and expressed in a common inertial reference frame. The heading and angular velocity are denoted by $(\theta_p, \omega_p) \in (-\pi, \pi] \times \mathbb{R}$, and the linear velocity is denoted by $v_p \in \mathbb{R}$. The control input of agent p is $\mu_p \triangleq (v_p, \omega_p) \in \mathbb{R}^2$.

For each marine craft $p \in \mathcal{V}$, let $\ell \in \mathbb{R}_{>0}$ denote the length between the CM and bow. Using the CM position c_p , heading θ_p , and length ℓ , the position of the bow of agent p is given by $b_p \triangleq c_p + \ell(\cos(\theta_p), \sin(\theta_p))$. Figure 2 provides a clarifying illustration. The goal of this simulation example is to achieve

rendezvous in the bow positions, that is, $b_p = b_q$ for all $p, q \in \mathcal{V}$. To enable the use of our consensus result, we introduce a transformation. Utilizing (70), the time derivative of b_p is

$$\dot{b}_p = \underbrace{\begin{bmatrix} \cos(\theta_p) & -\sin(\theta_p) \\ \sin(\theta_p) & \cos(\theta_p) \end{bmatrix}}_{\triangleq R(\theta_p)} \underbrace{\begin{bmatrix} 1 & 0 \\ 0 & \ell \end{bmatrix}}_{\triangleq D} \mu_p. \quad (71)$$

Since $R(\theta_p)$ is a rotation matrix and $\ell > 0$, $R(\theta_p)^{-1}$ and D^{-1} are always well-defined. Furthermore, for any velocity \dot{b}_p , the corresponding control input is given by $\mu_p = D^{-1}R(\theta_p)^{-1}\dot{b}_p$. Given a continuously differentiable reference trajectory for the bow position b_p , one can compute the corresponding control input for (70), pointwise in time, by utilizing the inverse map $T^{-1}(\theta_p, s) \triangleq D^{-1}R(\theta_p)^{-1}s$. Next, we provide a method for producing a reference trajectory for each b_p .

For each agent $p \in \mathcal{V}$, consider the auxiliary system

$$\mathbf{M}\ddot{z}_p + \mathbf{C}\dot{z}_p = u_p, \quad (72)$$

where $z_p \in \mathbb{R}^2$ denotes a virtual position, $u_p \in \mathbb{R}^2$ is a virtual control input, $\mathbf{M} \in \mathbb{R}^{2 \times 2}$ is a positive definite mass matrix, and $\mathbf{C} \in \mathbb{R}^{2 \times 2}$ is a non-zero viscous damping matrix. The second-order ODE in (72) can be expressed as an LTI system by using $x_{1,p} \triangleq z_p$, $x_{2,p} \triangleq \dot{z}_p$, $x_p \triangleq (x_{1,p}, x_{2,p})$, and

$$A \triangleq \begin{bmatrix} 0_{2 \times 2} & I_2 \\ 0_{2 \times 2} & -\mathbf{M}^{-1}\mathbf{C} \end{bmatrix}, \quad B \triangleq \begin{bmatrix} 0_{2 \times 2} \\ \mathbf{M}^{-1} \end{bmatrix}, \quad H \triangleq [I_2 \quad 0_{2 \times 2}]. \quad (73)$$

Note (A, B) is controllable, (A, H) is observable, and position is assumed measurable given the definition of H .

The ODE in (72) complies with the LTI model requirement of our consensus strategy and can model the motion of a point-mass under the influence of viscous damping. Furthermore, the ODE in (72) will be used to generate an almost-everywhere continuously differentiable reference trajectory for the bow of agent p , which will be tracked using $T^{-1}(\theta_p, x_{2,p})$. We now describe an implementation of this reference trajectory tracking strategy. Since $x_{1,q}$ is the virtual position variable of agent q , which is not a physical quantity that can be independently measured by agent $p \neq q$, the controller comprised of (6)–(10) is not directly implementable. Nevertheless, knowledge of $x_{1,q}$ can be granted via wireless communication and computation. For example, consider agent p . Whenever agent p updates η_p or ζ_{pr} for some $r \in [M^*]$, agent p can broadcast the updated quantity to all neighboring agents $q \in \mathcal{N}_p$. If $K_{\eta,p} = K_{\eta,q}$ and $K_{\zeta,pr} = K_{\zeta,qs}$ for all $p, q \in \mathcal{V}$ and $r, s \in [M^*]$ or if these matrices are distinct and known *a priori* by all agents, then η_p and ζ_{pr} can be computed independently and simultaneously by all neighbors of agent p given the flow dynamics in (8) and (9). Hence, each neighbor of agent p can compute the control input of agent p , where exact model knowledge of (72) enables each neighbor of agent p to compute $x_{1,p}$. By repeating this strategy for every neighbor $k \in \mathcal{N}_q$, agent q can implement (6)–(10) to obtain a reference trajectory for itself.

By driving the auxiliary variables in $\{x_p\}_{p \in \mathcal{V}}$ into consensus, which will be achieved using the result from Section IV, and applying the transformation T^{-1} , pointwise in continuous-time for each agent $p \in \mathcal{V}$, the marine crafts can accomplish rendezvous with respect to the bow positions. Two simulation

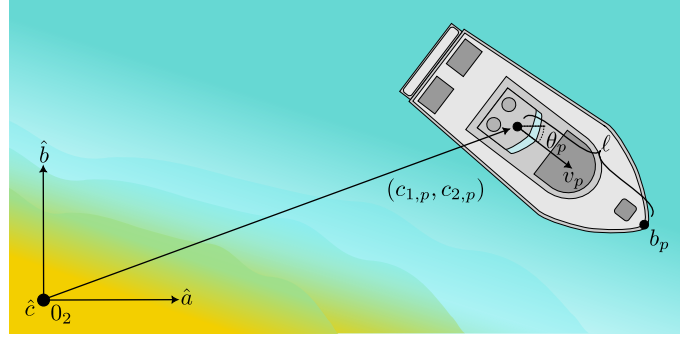


Figure 2: A common inertial reference frame is depicted on the bottom left with origin O_2 and right-handed coordinate system defined by the orthogonal unit vectors \hat{a} , \hat{b} , and \hat{c} . The positions of the CM and bow of agent p are given by c_p and b_p , respectively. The distance between the CM and bow is denoted by ℓ . The speed along the unit vector $(b_p - c_p)/\|b_p - c_p\|$ and heading relative of \hat{a} of agent p are denoted by v_p and θ_p , respectively.

cases are considered, namely, a nominal simulation that is free of perturbations and a more realistic simulation that contains measurement noise. The simulation parameters are $N = 14$, $n = 4$, $d = m = 2$, $M = 5$, $M^* = 8$, $\ell = 0.53$, $\sigma = 500$, $\mathbf{M} = I_2$, $\mathbf{C} = 2.66 \cdot I_2$, $K_u = 0.5 \cdot I_2$, and, for all $p \in \mathcal{V}$ and $r \in [M^*]$, $T_1^p = T_3^r = 0.001$, $T_2^p = T_4^r = 0.01$,

$$K_{\eta,p} = K_{\zeta,pr} = \begin{bmatrix} -2.33 & -1.33 \\ 1.33 & -5.66 \end{bmatrix}.$$

Moreover, $x_{1,p}(0,0) = b_p(0,0)$ for each $p \in \mathcal{V}$. Under these parameters, MATLAB and the CVX Toolbox [39], [40] were employed to solve the matrix inequality $\mathbf{M}(\tau, \rho) \leq \mathbf{0}$ for points $(\tau, \rho) = (0_N, 0_{M^*})$ and $(\tau, \rho) = (T_2, T_4)$. Consequently, Corollary 1 implies the sufficient conditions of Theorem 1 are satisfied. Unfortunately, we are unable to provide the solution to the matrix inequality since $P(0_N, 0_{M^*}) \in \mathbb{R}^{304 \times 304}$ in our application.

The parameters and communication topology, i.e., the clustered network depicted in Figure 3, are identical for the nominal and perturbed simulation cases. Figures 4–6 correspond to the simulation results for the nominal case, while Figures 7–8 correspond to the simulation results for the perturbed case. To examine the robustness of our consensus controller to various perturbation magnitudes and communication graphs, a modest Monte Carlo simulation was performed with results provided in Figure 9. Note only the graph \mathcal{G} , perturbation magnitudes, and controller matrix K_u were changed in the Monte Carlo simulation. The matrix $K_u = 1.5 \cdot I_2$ was fixed for all 30 runs of the Monte Carlo simulation. However, the graph \mathcal{G} and perturbation magnitudes were randomly selected from the set of connected graphs on N nodes and the interval $[0, 0.075]$ using a uniform distribution, respectively. The partition of each graph's node set \mathcal{V} was also randomly selected.

A. Consensus under Ideal Conditions

As validated by Figures 4–6, the proposed control strategy in Section IV renders the set \mathcal{A} globally exponentially stable under ideal conditions (i.e., under the absence of measurement noise). Consequently, the reference trajectories for the marine

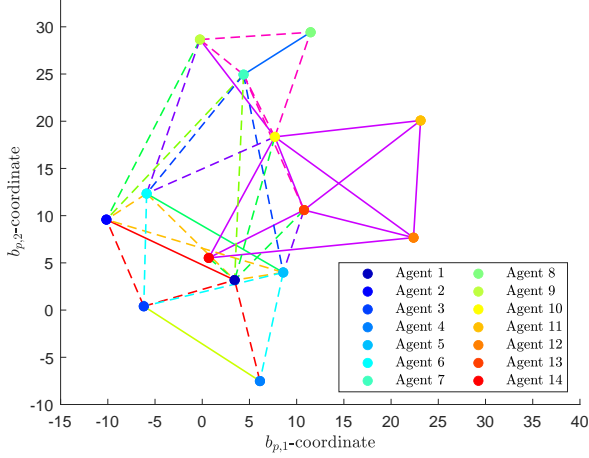


Figure 3: Illustration of the clustered network used in the nominal and perturbed simulation cases. The nodes and edges of the communication graph \mathcal{G} are represented by the disks and both solid and dashed lines, respectively. Different colored disks connected by solid lines of the same color represent a cluster sub-graph. Different colored disks connected by dashed lines of the same color represent an inter-cluster sub-graph. The planar position of each node is coincident with the initial bow position of the corresponding agent.

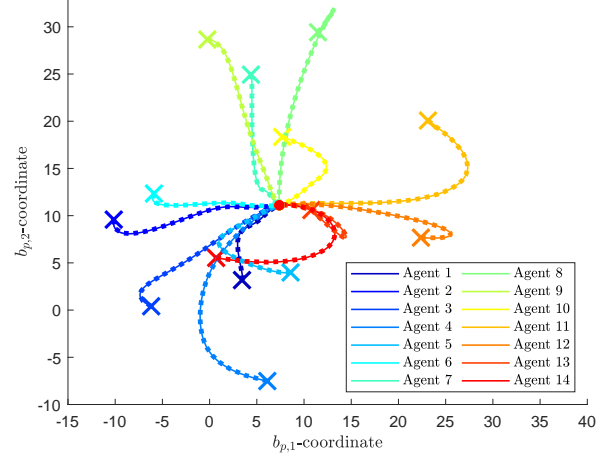


Figure 4: Illustration of the reference bow position trajectories and true bow position trajectories for each agent $p \in \mathcal{V}$. Solid lines represent the trajectories of $\{x_{1,p}\}_{p \in \mathcal{V}}$ (reference bow positions), while dotted lines represent the trajectories of $\{b_p\}_{p \in \mathcal{V}}$ (true bow positions). The 'x's and '•'s depict the initial and final conditions of all trajectories, respectively. Observe rendezvous is achieved in both the reference bow positions $\{x_{1,p}\}_{p \in \mathcal{V}}$ and true bow positions $\{b_p\}_{p \in \mathcal{V}}$.

crafts can be synchronized exponentially fast while using intermittent and asynchronous output feedback (that is, position measurements). Also, the map $(\theta_p, x_{2,p}) \mapsto D^{-1}R(\theta_p)^{-1}x_{2,p}$ enabled each agent $p \in \mathcal{V}$ to track their reference trajectory. Recall $x_{2,p}$ denotes the velocity of the reference trajectory for agent p . Therefore, we were able to achieve exponentially fast rendezvous for marine crafts modeled by (70).

Of course, driving $|\xi|_{\mathcal{A}}$ to 0 in practice would probably be undesirable as the user may not wish for potentially expensive marine crafts to crash into each other. Thus, achieving $|\xi|_{\mathcal{A}} \leq \omega$ for some appropriate $\omega > 0$ may suffice instead. Given such a scenario, $|\xi|_{\mathcal{A}} \leq \omega$, (34), and (41) facilitate the calculation of a conservative, albeit finite, continuous time for achieving ω -approximate rendezvous (see [41, Definition 2]). In particular,

$$\left. \begin{aligned} t^* \triangleq \frac{2\alpha_2}{\mu} \ln \left(\sqrt{\frac{\alpha_2}{\alpha_1}} \frac{|\phi(0,0)|_{\mathcal{A}}}{\omega} \right) \leq t \\ 0 < \omega < \sqrt{\frac{\alpha_2}{\alpha_1}} |\phi(0,0)|_{\mathcal{A}} \end{aligned} \right\} \implies |\phi(t,j)|_{\mathcal{A}} \leq \omega$$

for all $(t,j) \in \text{dom } \phi$ such that $(t,j) \geq (t^*,j^*)$ with $(t^*,j^*) \in \text{dom } \phi$. The time t^* denotes when ω -approximate rendezvous is guaranteed to occur, which depends on the initial condition and control parameters. The inequality constraint on ω ensures the logarithm above is positive, yielding a well-defined future time t^* . While the nominal simulation provides good results, non-vanishing measurement noise will affect a cyber-physical system in practice. Ergo, the following simulation is motivated.

B. Consensus under Measurement Noise

To simulate non-vanishing measurement noise, we employ the following: for all $p \in \mathcal{V}$ and $r \in [M^*]$, let

$$\begin{aligned} \delta_p &= 0.07 \sin(0.015t) \sin(0.2t) \cdot 1_m \\ \delta_{pr} &= 0.04 \sin(0.095t) \cos(0.4t) \cdot 1_m, \end{aligned} \quad (74)$$

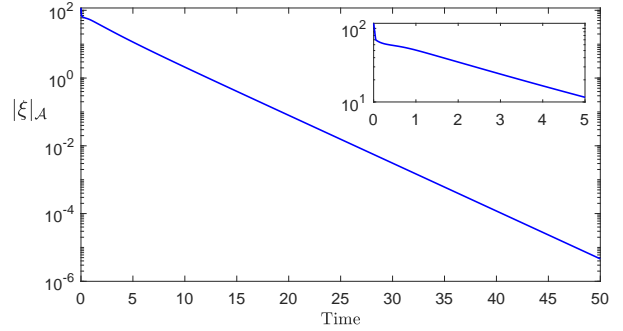


Figure 5: Depiction of $|\xi|_{\mathcal{A}}$ as a function of continuous time, where $\xi = \phi(t,j)$ —the particular solution to the hybrid system \mathcal{H} generated in the nominal simulation. The vertical axis uses a logarithmic scale; the horizontal axis uses a linear scale. Based on the plot, the distance of ξ to \mathcal{A} is exponentially converging to 0.

where the perturbations δ_p and δ_{pr} are explicit functions of continuous time. Although all agents are subjected to the same perturbations, the induced affects are different because agents introduce samples of these perturbations are different moments in time, potentially, given the jump map in (54).

With respect to Figures 7–8, the non-vanishing measurement noise has a clear effect on the trajectories of the MAS. Minor oscillations in the rendezvous point, $\tilde{\eta}_p$ for all $p \in \mathcal{V}$, $\tilde{\zeta}_r$ for all $r \in [M^*]$, and $|\xi|_{\mathcal{A}}$ are apparent. Nevertheless, ω -approximate rendezvous is accomplished for $\omega \leq 1 \times 10^{-4}$.

To further examine the robustness of the consensus result to measurement noise, 30 additional simulations using randomly selected clustered networks and perturbation magnitudes were conducted. Nearly all simulation parameters were unchanged, except $K_u = 1.5 \cdot I_2$. Figure 9 shows the results of these simulations. In all cases, ω -approximate rendezvous was achieved.

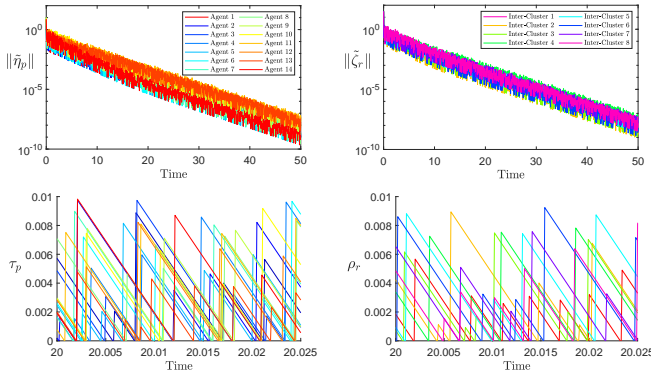


Figure 6: (Top Left) Depiction of $\|\tilde{\eta}_p(\phi(t, j))\|$, for each agent $p \in \mathcal{V}$, versus continuous time. Note that the vertical axis uses a logarithmic scale, while the horizontal axis uses a linear scale. Although noisy, the magnitude of $\tilde{\eta}_p$, along the solution $\phi(t, j)$, tends to 0 as $t + j$ approaches infinity. **(Bottom Left)** Depiction of the trajectories of $\tau_p(\phi(t, j))$ for each $p \in \mathcal{V}$. Since τ_p determines when agent p updates the η_p component of its controller (i.e., when $\tau_p = 0$) and the timers in $\{\tau_q\}_{q \in \mathcal{V}}$ reach 0 at different times, the variables in $\{\eta_q\}_{q \in \mathcal{V}}$ are updated intermittently and asynchronously with respect to each other. **(Top Right)** Depiction of $\|\tilde{\zeta}_r(\phi(t, j))\|$, for each $r \in [M^*]$, versus continuous time. Note that the vertical axis uses a logarithmic scale, while the horizontal axis uses a linear scale. Although noisy, the magnitude of $\tilde{\zeta}_r$, along the solution $\phi(t, j)$, tends to 0 as $t + j$ approaches infinity. **(Bottom Right)** Depiction of the trajectories of $\rho_r(\phi(t, j))$ for each $r \in [M^*]$. Since ρ_r determines when the agents in inter-cluster r update the ζ_{qr} component of their controller, for $q \in \mathcal{V}^r$, and the timers in $\{\rho_s\}_{s \in \mathcal{V}^r}$ reach 0 at different times, the variables in $\{\zeta_{qr}\}_{q \in \mathcal{V}^r}$ are updated intermittently and asynchronously with respect to the variables in $\{\zeta_{qs}\}_{q \in \mathcal{V}^s}$ for $r \neq s \in [M^*]$. Note that, for each $p \in \mathcal{V}$, the color of $\|\tilde{\eta}_p\|$ matches that of τ_p . Likewise, for each $r \in [M^*]$, the color of $\|\tilde{\zeta}_r\|$ matches that of ρ_r .

VIII. CONCLUSION

This paper develops a distributed consensus controller for clustered network of LTI systems using intermittent and asynchronous output feedback. The controller consists of multiple components that are intermittently updated with output information from neighbors of the same cluster and potentially multiple inter-clusters at different rates. Despite the clustered graph structure, which may result in disconnected distanced-based communication graphs as modeled through the timer dynamics, the MAS can still achieve system-wide consensus.

Future work may consider nonlinear, uncertain, and/or heterogeneous agent models. One may examine consensus under path constraints to guarantee safety or other desired behaviors. More advanced observers can also be developed to promote even less frequent communication and/or measurements.

REFERENCES

- [1] Z. Li, Z. Hu, and C. Li, *SRv6 Network Programming: Ushering in a New Era of IP Networks*. CRC Press, 2021.
- [2] C. Chang, S. N. Srirama, and R. Buyya, "Internet of Things (IoT) and New Computing Paradigms," *Fog and Edge Computing: Principles and Paradigms*, vol. 6, pp. 1–23, 2019.
- [3] L. Wang and Y. Xiao, "A Survey of Energy-Efficient Scheduling Mechanisms in Sensor Networks," *Mobile Networks and Applications*, vol. 11, no. 5, pp. 723–740, 2006.
- [4] F. Zaidi, "Small World Networks and Clustered Small World Networks

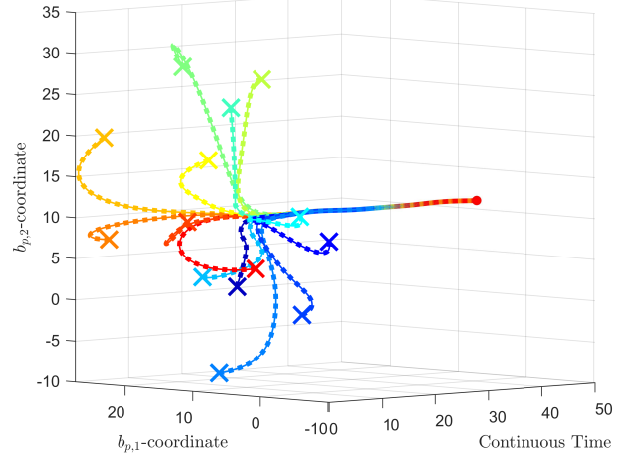


Figure 7: Illustration of the reference bow position trajectories and true bow position trajectories for each agent $p \in \mathcal{V}$. Solid lines represent the trajectories of $\{x_{1,p}\}_{p \in \mathcal{V}}$ (reference bow positions), while dotted lines represent the trajectories of $\{b_p\}_{p \in \mathcal{V}}$ (true bow positions). The \times 's and \bullet 's depict the initial and final conditions of all trajectories, respectively. Observe rendezvous is achieved in both the reference bow positions $\{x_{1,p}\}_{p \in \mathcal{V}}$ and true bow positions $\{b_p\}_{p \in \mathcal{V}}$ despite the presence of measurement noise. Nevertheless, unlike the nominal simulation, the rendezvous point moves slightly under the influence of measurement noise.

- with Random Connectivity," *Social Network Analysis and Mining*, vol. 3, pp. 51–63, 2013.
- [5] Q. K. Telesford, K. E. Joyce, S. Hayasaka, J. H. Burdette, and P. J. Laurienti, "The Ubiquity of Small-World Networks," 2011.
- [6] D. J. Watts and S. H. Strogatz, "Collective Dynamics of 'Small-World' Networks," *Nature*, vol. 393, no. 6684, pp. 440–442, 1998.
- [7] M. Mesbahi and M. Egerstedt, *Graph Theoretic Methods in Multiagent Networks*. Princeton University Press, 2010.
- [8] R. Olfati-Saber, J. A. Fax, and R. M. Murray, "Consensus and Cooperation in Networked Multi-Agent Systems," *Proceedings of the IEEE*, vol. 95, no. 1, pp. 215–233, 2007.
- [9] J. Qin, Q. Ma, Y. Shi, and L. Wang, "Recent Advances in Consensus of Multi-Agent Systems: A Brief Survey," *IEEE Transactions on Industrial Electronics*, vol. 64, no. 6, pp. 4972–4983, 2017.
- [10] Y. Li and C. Tan, "A Survey of the Consensus for Multi-Agent Systems," *Systems Science & Control Engineering*, vol. 7, no. 1, pp. 468–482, 2019.
- [11] A. Dorri, S. S. Kanhere, and R. Jurdak, "Multi-Agent Systems: A Survey," *IEEE Access*, vol. 6, pp. 28 573–28 593, 2018.
- [12] L. Ding, Q.-L. Han, X. Ge, and X.-M. Zhang, "An Overview of Recent Advances in Event-Triggered Consensus of Multiagent Systems," *IEEE Transactions on Cybernetics*, vol. 48, no. 4, pp. 1110–1123, 2017.
- [13] C. Nowzari, E. Garcia, and J. Cortes, "Event-Triggered Communication and Control of Networked Systems for Multi-Agent Consensus," *Automatica*, vol. 105, pp. 1–27, 2019.
- [14] X. Ge and Q.-L. Han, "A Brief Survey of Recent Advances in Consensus of Sampled-Data Multi-Agent Systems," in *Proceedings of the Conference of the IEEE Industrial Electronics Society*, 2016, pp. 6758–6763.
- [15] S. Phillips and R. G. Sanfelice, "Pointwise Exponential Stability of State Consensus with Intermittent Communication," *IEEE Transactions on Automatic Control*, pp. 1–16, 2024.
- [16] F. M. Zegers, D. P. Guralnik, S. C. Edwards, C.-L. Lee, and W. E. Dixon, "Event-Triggered Consensus for Second-Order Systems: A Hybrid Systems Perspective," in *Proceedings of Conference on Decision and Control*, 2022, pp. 427–434.
- [17] S. Phillips and R. G. Sanfelice, "Robust Distributed Synchronization of Networked Linear Systems with Intermittent Information," *Automatica*, vol. 105, pp. 323–333, 2019.
- [18] F. M. Zegers, D. P. Guralnik, and W. E. Dixon, "Event-Triggered Multi-Agent System Rendezvous with Graph Maintenance in Varied Hybrid

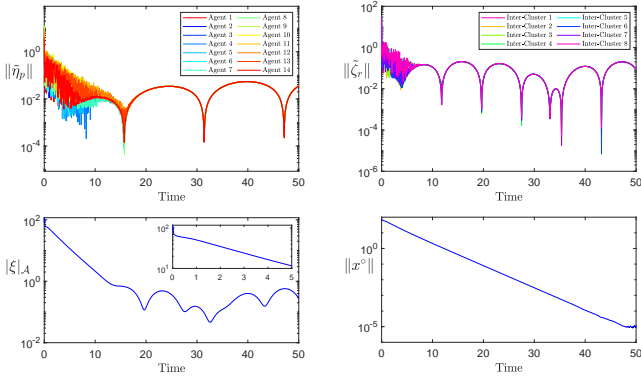


Figure 8: (Top Left) Depiction of $\|\tilde{\eta}_p(\phi(t, j))\|$, for each $p \in \mathcal{V}$, versus continuous time. Note the vertical axis uses a logarithmic scale, while the horizontal axis uses a linear scale. The large oscillations in the trajectories are caused by the sinusoidal measurement noise. (Bottom Left) Illustration of the trajectory of $|\xi|_{\mathcal{A}}$, where $\xi = \phi(t, j)$ —the particular solution to the hybrid system \mathcal{K} generated in the simulation. Observe that the measurement noise causes ξ to converge to an ω -fattening of \mathcal{A} for some constant $\omega \in \mathbb{R}_{>0}$. (Top Right) Depiction of $\|\tilde{\zeta}_r(\phi(t, j))\|$, for each $r \in [M^*]$, versus continuous time. Observe that the vertical axis uses a logarithmic scale, while the horizontal axis uses a linear scale. The large oscillations in the trajectory are due to the sinusoidal measurement noise. (Bottom Right) Illustration of $\|x^\circ(\phi(t, j))\|$ versus continuous time. Despite the presence of measurement noise, the disagreement in $\{x_p\}_{p \in \mathcal{V}}$ can be made small and oscillates around a magnitude of 1×10^{-5} .

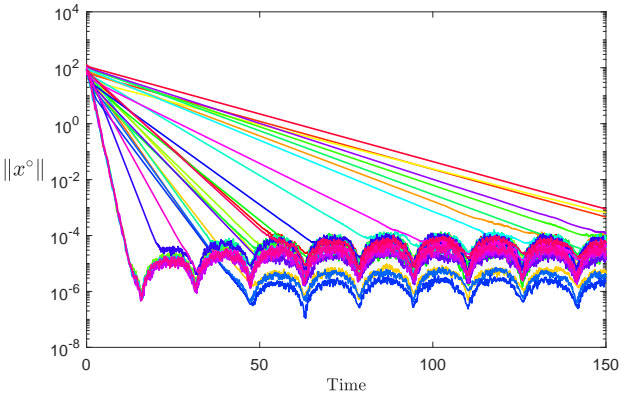


Figure 9: Illustration of $\|x^\circ(\phi(t, j))\|$ versus continuous time for 30 different simulations. Each color corresponds to a unique scenario and a distinct solution ϕ to \mathcal{K} . Nearly all simulation parameters are unchanged between runs except for the clustered network and perturbation magnitude. In all cases, the MAS drove $\|x^\circ(\phi(t, j))\|$ to a small neighborhood of 0.

Formulations: A Comparative Study,” *IEEE Transactions on Automatic Control*, pp. 1–15, 2024.

- [19] Y. Fan, Y. Yang, and Y. Zhang, “Sampling-Based Event-Triggered Consensus for Multi-Agent Systems,” *Neurocomputing*, vol. 191, pp. 141–147, 2016.
- [20] P. Wirasanti, E. Ortjohann, A. Schmelter, and D. Morton, “Clustering Power Systems Strategy the Future of Distributed Generation,” in *International Symposium on Power Electronics, Electrical Drives, Automation and Motion*, 2012, pp. 679–683.
- [21] X. Cheng and J. M. A. Scherpen, “Clustering Approach to Model Order Reduction of Power Networks with Distributed Controllers,” *Advances in Computational Mathematics*, vol. 44, no. 6, pp. 1917–1939, 2018.
- [22] R. J. Sánchez-García, M. Fennelly, S. Norris, N. Wright, G. Niblo, J. Brodzki, and J. W. Bialek, “Hierarchical Spectral Clustering of Power

Grids,” *IEEE Transactions on Power Systems*, vol. 29, no. 5, pp. 2229–2237, 2014.

- [23] S. Bandyopadhyay and E. J. Coyle, “Minimizing Communication Costs in Hierarchically-Clustered Networks of Wireless Sensors,” *Computer Networks*, vol. 44, no. 1, pp. 1–16, 2004.
- [24] I. Jayawardene, P. Herath, and G. K. Venayagamoorthy, “A Graph Theory-Based Clustering Method for Power System Networks,” in *Proceedings of Clemson University Power Systems Conference*, 2020, pp. 1–8.
- [25] J. Qin and C. Yu, “Cluster Consensus Control of Generic Linear Multi-Agent Systems under Directed Topology with Acyclic Partition,” *Automatica*, vol. 49, no. 9, pp. 2898–2905, 2013.
- [26] X. Ge, Q.-L. Han, and X.-M. Zhang, “Achieving Cluster Formation of Multi-Agent Systems Under Aperiodic Sampling and Communication Delays,” *IEEE Transactions on Industrial Electronics*, vol. 65, no. 4, pp. 3417–3426, 2018.
- [27] V. T. Pham, N. Messai, and N. Manamanni, “Impulsive Observer-Based Control in Clustered Networks of Linear Multi-Agent Systems,” *IEEE Transactions on Network Science and Engineering*, vol. 7, no. 3, pp. 1840–1851, 2020.
- [28] V. T. Pham, N. Messai, D. H. Nguyen, and N. Manamanni, “Robust Formation Control under State Constraints of Multi-Agent Systems in Clustered Networks,” *Systems & Control Letters*, vol. 140, p. 104689, 2020.
- [29] S. Luo and D. Ye, “Cluster Consensus Control of Linear Multiagent Systems Under Directed Topology With General Partition,” *IEEE Transactions on Automatic Control*, vol. 67, no. 4, pp. 1929–1936, 2022.
- [30] F. M. Zegers, S. Phillips, and W. E. Dixon, “Consensus over Clustered Networks with Asynchronous Inter-Cluster Communication,” in *Proceedings of American Control Conference*, 2021, pp. 4249–4254.
- [31] C. F. Nino, F. M. Zegers, S. Phillips, and W. E. Dixon, “Consensus over Clustered Networks Using Output Feedback and Asynchronous Inter-Cluster Communication,” in *Proceedings of American Control Conference*, 2023, pp. 4844–4851.
- [32] R. Goebel, R. G. Sanfelice, and A. R. Teel, *Hybrid Dynamical Systems: Modeling, Stability, and Robustness*. Princeton University Press, 2012.
- [33] A. R. Teel, F. Forni, and L. Zaccarian, “Lyapunov-Based Sufficient Conditions for Exponential Stability in Hybrid Systems,” *IEEE Transactions on Automatic Control*, vol. 58, no. 6, pp. 1591–1596, 2013.
- [34] Y. Li, S. Phillips, and R. G. Sanfelice, “Robust Distributed Estimation for Linear Systems Under Intermittent Information,” *IEEE Trans. Autom. Control*, vol. 63, pp. 973–988, 2018.
- [35] C. Cai and A. R. Teel, “Characterizations of Input-To-State Stability for Hybrid Systems,” *Systems & Control Letters*, vol. 58, no. 1, pp. 47–53, 2009.
- [36] F. M. Zegers, S. Phillips, and G. P. Hicks, “Timer-Based Coverage Control for Mobile Sensors,” *ArXiv*, Feb. 2024. [Online]. Available: <https://arxiv.org/abs/2402.18744>
- [37] L. Rodrigues, “From LQR to Static Output Feedback: A New LMI Approach,” in *Proceedings of IEEE Conference on Decision and Control*, 2022, pp. 4878–4883.
- [38] S. Phillips and R. G. Sanfelice, “Robust Distributed Synchronization of Networked Linear Systems with Intermittent Information,” *Automatica*, vol. 105, pp. 323–333, 2019.
- [39] M. Grant and S. Boyd, “Graph Implementations for Nonsmooth Convex Programs,” in *Recent Advances in Learning and Control*. Springer-Verlag Limited, 2008, pp. 95–110.
- [40] —, “CVX: Matlab Software for Disciplined Convex Programming, version 2.1,” <https://cvxr.com/cvx>, Mar. 2014.
- [41] F. M. Zegers, D. P. Guralnik, and W. E. Dixon, “Event/Self-Triggered Multi-Agent System Rendezvous with Graph Maintenance,” in *Proceedings of IEEE Conference Decision and Control*, 2021.

APPENDIX A PROOF OF LEMMA 1

Since the graph \mathcal{G} is undirected and defined on N nodes, the associated Laplacian matrix $L \in \mathbb{R}^{N \times N}$ is symmetric, which implies L is diagonalizable and has real eigenvalues. Further, since \mathcal{G} is static, the diagonalization of L is fixed. Let $\gamma \triangleq \{w_1, w_2, \dots, w_N\} \subset \mathbb{R}^N$ and $\{\lambda_1, \lambda_2, \dots, \lambda_N\} \subset \mathbb{R}$ denote the eigenvector and eigenvalue sets of L , respectively, where λ_p is the eigenvalue corresponding to eigenvector w_p for each $p \in [N]$. Since \mathcal{G} is connected, $w_1 \in \text{Span}(1_N)$, $\lambda_1 = 0$, and,

without loss of generality, $\lambda_1 < \lambda_2 \leq \dots \leq \lambda_N$. Observe that γ is an ordered basis for $\text{Range}(L)$. We can then employ the Gram-Schmidt process on γ to construct an orthogonal basis $\beta' = \{v'_1, v'_2, \dots, v'_N\}$ for $\text{Range}(L)$, where the normalization of the elements in β' yields an orthonormal basis β . That is, $\beta = \{v_1, v_2, \dots, v_N\} \subset \mathbb{R}^N$, where $v_p \triangleq v'_p / \|v'_p\|$ and $v_p \perp v_q$ for all distinct $p, q \in [N]$. Observe β' and β are not necessarily unique. Since $w_1 \in \text{Span}(1_N)$, $w_1 = c \cdot 1_N$ for some constant $c \in \mathbb{R} \setminus \{0\}$. Since the Gram-Schmidt process allows for $v'_1 \triangleq |w_1|$, it follows that $v_1 = |c| \cdot 1_N / \|c \cdot 1_N\| = (\sqrt{N}/N) \cdot 1_N$.

Using the elements in β , let $V' \triangleq [v_1, v_2, \dots, v_N] \in \mathbb{R}^{N \times N}$. Similarly, let $D' \triangleq \text{diag}(\lambda_1, \lambda_2, \dots, \lambda_N) \in \mathbb{R}^{N \times N}$. Recall $\lambda_1 = 0$ and $\lambda_p > 0$ for every $p = 2, 3, \dots, N$. Moreover, $(V')^{-1} = (V')^\top$ since the columns of V' form an orthonormal set. Using the diagonalization of L , one has that⁹

$$\begin{aligned} L &= V'D'(V')^{-1} = V'D'(V')^\top \\ &= \sum_{p \in [N]} \lambda_p v_p v_p^\top = \lambda_1 v_1 v_1^\top + \sum_{p \in [N] \setminus \{1\}} \lambda_p v_p v_p^\top \\ &= VDV^\top, \end{aligned}$$

such that $D = \text{diag}(\lambda_2, \lambda_3, \dots, \lambda_N) \in \mathbb{R}^{(N-1) \times (N-1)}$ is a positive definite matrix. Recall \tilde{e}_k denotes the k^{th} standard basis vector of \mathbb{R}^{N-1} . Since the columns of V are pairwise orthogonal, one has that $V^\top v_p = \tilde{e}_{p-1}$ for all $p = 2, 3, \dots, N$. Therefore,

$$V^\top V = [V^\top v_2, V^\top v_3, \dots, V^\top v_N] = I_{N-1}.$$

Lastly, recall $S = I_N - 1_N 1_N^\top / N$. Note $V'(V')^\top = I_N$ since V' is an orthonormal matrix. It then follows that

$$\begin{aligned} VV^\top &= \sum_{p \in [N] \setminus \{1\}} v_p v_p^\top + \sum_{p \in [N] \setminus \{1\}} v_p v_p^\top + v_1 v_1^\top - v_1 v_1^\top \\ &= \sum_{p \in [N]} v_p v_p^\top - \frac{\sqrt{N}}{N} 1_N \frac{\sqrt{N}}{N} 1_N^\top \\ &= V'(V')^\top - \frac{1}{N} 1_N 1_N^\top = S. \end{aligned}$$

Hence, the desired result follows. \blacksquare

APPENDIX B PROOF OF LEMMA 3

Item 1: The proof is based on [32, Proposition 2.10]. Observe that the flow map f in (24) is globally Lipschitz. Consider the differential equation $\dot{\xi} = f(\xi)$ with initial condition $\phi(0, 0) \in C \setminus D$. Then, there exists a nontrivial, maximal solution ϕ for \mathcal{H} satisfying the initial condition. Further, under the construction of \mathcal{H} , $G(D) \subset C \cup D$ implying that Item (c) in [32, Proposition 2.10] does not occur. Because the single-valued flow map f is Lipschitz continuous, Item (b) in [32, Proposition 2.10] does not occur. Hence, ϕ is complete.

Item 2: The following is guided by the proof of Lemma 3.5 in [34]. Fix a maximal solution ϕ of \mathcal{H} , and let $(t', j') \in \text{dom } \phi$.

Case I: Suppose $(t, j) \in \text{dom } \phi$ such that $0 \leq t - t' \leq T_{\min}$ and $0 \leq j - j'$. With respect to the dynamics in (6) and (7), at

most $N + M^*$ timers may jump twice during a flow interval of length T_{\min} . This occurs when $\tau_p(t', j') = 0$ with $\tau_p^+ = T_{\min}$ for each $p \in \mathcal{V}$ and $\rho_r(t', j') = 0$ with $\rho_r^+ = T_{\min}$ for each $r \in [M^*]$.¹⁰ If a timer has a value in $(0, T_{\min}]$ at time (t', j') , then that timer jumps once during a flow interval of length T_{\min} . Hence, the number of jumps between (t', j') and (t, j) is bounded as $j - j' \leq (N + M^*) \left(\frac{t - t'}{T_{\min}} + 1 \right)$, which implies that

$$\left(\frac{j - j'}{N + M^*} - 1 \right) T_{\min} \leq t - t'. \quad (75)$$

Case II: Suppose $(t, j) \in \text{dom } \phi$ such that $t - t' = T_{\max}$ and $0 \leq j - j'$. With respect to the dynamics in (6) and (7), at least $N + M^*$ timers must jump once during a flow interval of length T_{\max} . This occurs when $\tau_p(t', j') = T_{\max}$ for each $p \in \mathcal{V}$ and $\rho_r(t', j') = T_{\max}$ for each $r \in [M^*]$.¹⁰ If a timer has a value of 0 at time (t', j') and is reset to some value in $[T_{\min}, T_{\max}]$, then that timer may jump at least twice during a flow interval of length T_{\max} . Hence, the number of jumps between (t', j') and (t, j) is bounded as $(N + M^*) \frac{t - t'}{T_{\max}} \leq j - j'$, which implies that

$$t - t' \leq \frac{j - j'}{N + M^*} T_{\max}. \quad (76)$$

Combining (75) and (76) while setting $(t', j') = (0, 0)$ yields the result in (29). \blacksquare



Federico M. Zegers (Member, IEEE) received a B.S. in Mechanical Engineering in 2016, a B.S. in Mathematics in 2016, an M.S. in Mechanical Engineering in 2019, and a Ph.D. in Mechanical Engineering in 2021 from the University of Florida, Gainesville, FL, USA. He is currently a Senior Professional Staff I within the Air and Missile Defense Sector of Johns Hopkins University Applied Physics Laboratory, Laurel, MD, USA. His research focuses on Lyapunov-based nonlinear and adaptive control, switched and hybrid systems, multi-agent systems,

and robotics.



Sean Phillips (M'11) received his B.S. and M.S. degrees in Mechanical Engineering from the University of Arizona, Tucson, Arizona, in 2011 and 2013, respectively. In 2018, he received a Ph.D. in Computer Engineering from the University of California – Santa Cruz, California. He is a Research Mechanical Engineer and Technology Advisor of the Space Control Branch at the Air Force Research Laboratory in the Space Vehicles Directorate. He also holds the title of Research Assistant Professor (LAT) at the University of New Mexico in Albuquerque, NM. In

2009, he joined the Hybrid Dynamics and Controls Lab where he received a NASA Space Grant in 2010. In 2010, he received an Undergraduate Research Grant from the University of Arizona Honors College. He received a Space Scholars Internship at the Air Force Research Laboratory in Albuquerque N.M. during the summers of 2011, 2012, and 2017. In 2014, he joined the Hybrid Systems Laboratory at the University of California, Santa Cruz. In 2017, he received the Jack Baskin and Peggy Downes-Baskin Fellowship for his research on autonomous networked systems from the Baskin School of Engineering at the University of California Santa Cruz.

⁹The Gram-Schmidt process and normalization do not affect the bases of the eigenspaces of L . Hence, $\{w_p, \lambda_p\}_{p \in \mathcal{V}}$ and $\{v_p, \lambda_p\}_{p \in \mathcal{V}}$ yield different diagonalizations of L .

¹⁰ Such a reset is possible when $T_1^p = T_3^r$ and $T_2^p = T_4^r$ for all $p \in \mathcal{V}$ and $r \in [M^*]$.